Uncovering the Redundancy in Transformers via a Unified Study of Layer Dropping

Anonymous authors
Paper under double-blind review

Abstract

While scaling Transformer-based large language models (LLMs) has demonstrated promising performance across various tasks, it also introduces redundant architectures, posing efficiency challenges for real-world deployment. Despite some recognition of redundancy in LLMs, the variability of redundancy across different architectures in transformers, such as MLP and Attention layers, is under-explored. In this work, we investigate redundancy across different Transformer modules, including blocks, MLP layers, and attention layers, through the lens of layer dropping. Surprisingly, despite the pivotal role of attention mechanisms in distinguishing Transformers from other architectures, we find that a large portion of attention layers exhibit excessively high redundancy and can be pruned without degrading performance. For example, LLaMA-3-70B achieves a 43.4% speedup with only a 1.8% drop in performance by pruning half of its attention layers. In contrast, dropping MLP layers severely impairs the model's ability to distinguish between tokens, leading to catastrophic performance degradation. Moreover, our analysis reveals that attention layer redundancy persists not only throughout training but is also evident in randomly initialized models. We attribute this redundancy to three key factors that constrain representational updates from attention layers: sparse attention patterns, over-smoothed token embeddings, and the low representational magnitude of attention outputs. Overall, our findings offer valuable insights into the internal redundancy of Transformer architectures and provide practical guidance for designing more efficient LLMs. Code will be released upon acceptance.

1 Introduction

Transformer-based large language models (LLMs) have significantly advanced AI research, achieving remarkable performance across various domains (OpenAI, 2024; Team, 2024). However, scaling these models also introduces redundant architectures, namely overarching, leading to inefficiencies that complicate their real-world deployment (Frantar et al., 2023; Sun et al., 2023), e.g., inflating deployment costs and resource demands. Although several previous works have been proposed to promote LLM efficiency via removing redundant parameters or architectures (Frantar et al., 2023; Sun et al., 2023), these approaches often employ universal techniques that overlook the unique characteristics of transformer architectures. Specifically, transformer (Vaswani, 2017) architectures are composed of multiple stacked blocks, each containing an MLP layer and an Attention layer, which serve distinct functions and exhibit corresponding different levels of redundancy (Wang et al., 2023; Shi et al., 2023) This motivates a deeper investigation into the specific redundancies within Transformers, with the goal of identifying and addressing the most critical modules.

In this work, we systematically explore the redundancy in three key Transformer components: *Block*, *MLP*, and *Attention*. Using a similarity-based metric (Gromov et al., 2024; Men et al., 2024) , we evaluate the importance of each component and progressively drop those identified as redundant. We first apply a "*Block Drop*" approach but observe that removing entire blocks leads to significant performance degradation. This suggests a need for a more fine-grained strategy.

Upon further examination, we explore the separate pruning of MLP and Attention layers. Our findings reveal that while dropping MLP layers negatively affects performance, a substantial portion of Attention layers,

i.e., the core of Transformer architectures which distinguish it from other mainstream architectures (e.g., RWKV (Peng et al., 2023b) and Mamba (Gu & Dao, 2024)), can be pruned without degrading the model's performance. For instance, dropping 50% of the Attention layers in Llama-3-70B (Touvron et al., 2023) results in comparable performance to the full model, indicating a high degree of redundancy in these layers.

Our work provides a unified analysis of two key architectural components in Transformers: MLP and attention layers. On the one hand, MLP layers, which perform token transformations in high-dimensional space, contribute significantly to the hidden state representations. Without them, Transformer models suffer degraded sensitivity to token distinctions, resulting in substantial performance loss. In contrast, attention layers display notable redundancy. This redundancy persists across various training stages and is even observable in randomly initialized models, indicating that it is an inherent property of the architecture. We attribute this phenomenon to three key factors in attention architectures: (1) the sparsity of attention matrices, (2) the excessively high similarity between token embeddings, and (3) the low representational magnitude of the attention branch. These factors collectively constrain the representational updates contributed by attention layers to the residual branch, thereby making certain attention layers amenable to pruning. These findings offer valuable insights into the internal redundancy of Transformer architectures and provide practical guidance for designing more efficient LLMs. In summary, our key contributions are as follows:

- Through an in-depth analysis of redundancy in three key Transformer components, we uncover a surprising level of redundancy within the *Attention*.
- We propose *Attention Drop*, a simple yet effective algorithm for removing less important attention layers in a training-free manner, significantly improving efficiency without sacrificing performance.
- Our extensive experiments demonstrate the effectiveness of dropping Attention, for instance, removing 50% of the attention layers in Llama-3-70B results in only a 1.8% performance reduction while achieving up to a 43.4% speedup.
- We further demonstrate that attention layers possess inherent properties that lead to consistently high redundancy, both at initialization and throughout the training process. This observation offers valuable insights for future architectural design.

2 Related Works

Large Language Models Although Transformer-based Large Language Models (LLMs) have demonstrated promising performance across various tasks, their deployment costs still remain a significant challenge for practical usage (Sun et al., 2023; Lin et al., 2024; Gromov et al., 2024). Transformer (Vaswani, 2017) models consist of multiple blocks, which include Attention layers and MLP layers. Attention layers compute the contextual information between input tokens with quadratic complexity concerning the input sequence length (Li et al., 2020). KV-Cache (Pope et al., 2022) mitigates the computational issue but results in excessive memory costs (Zhang et al., 2023). MLP layers (Liu et al., 2021; Mai et al., 2022) transform each token independently, using an up-projection followed by a down-projection, and contribute most of the model parameters. Recent works have revealed that not all blocks or layers are equally important (Men et al., 2024; Chen et al., 2024), which urges us to reflect on the structured redundancy within LLMs and the potential design of more compact architectures.

Model Compression LLMs can be compressed to promote their efficiency in memory and computation. Quantization (Frantar et al., 2023; Lin et al., 2024) and Pruning (Sun et al., 2023; Frantar & Alistarh, 2023) are the most widely used techniques to compress LLMs. Specifically, quantization transforms the data type into low-bit but remains potentially redundant architecture and parameters. Pruning can be categorized into unstructured pruning (Kusupati et al., 2020; Sanh et al., 2020) and structured pruning (Zhuang et al., 2020; Kwon et al., 2020). While unstructured pruning maintains better performance than structured pruning, it cannot be effectively applied to hardware, limiting its practical usage. Our methods, Block Drop and Layer Drop, focus on removing structured modules rather than fine-grained parameters, creating hardware-friendly efficient architectures while maintaining comparable performance. Additionally, Block Drop and Layer Drop are orthogonal to quantization, and their integration with quantization significantly enhances efficiency.

3 Methodology

In this section, we present the methodology for identifying and removing redundant modules in LLMs. We begin by introducing a similarity-based metric to assess redundancy for layer importance. Based on the insights gained from this analysis, we develop two targeted techniques, i.e., MLP Drop and Attention Drop, to efficiently eliminate redundant components while preserving model performance.

3.1 Preliminaries

Similarity-based Drop To assess the redundancy of modules in LLMs, we employ a similarity-based metric that evaluates the importance of each module by measuring the similarity between its input and output (Gromov et al., 2024). The underlying hypothesis is that redundant modules produce outputs that are similar to their inputs, implying minimal transformation. In contrast, important modules are expected to significantly alter their inputs and thus should be preserved. The similarity between the hidden states of the input $\boldsymbol{X}$ and output $\boldsymbol{Y}$ of a module is quantified using cosine similarity. The importance score $\boldsymbol{S}$ of the module is computed as:

$$\boldsymbol{S} = 1 - \text{CosineSim}(\boldsymbol{X}, \boldsymbol{Y}). \tag{1}$$

Modules with higher cosine similarity exhibit lower importance scores, indicating redundancy. We identify and prune the modules with the lowest importance scores according to a predefined prunting ratio. A complete evaluation of the effectiveness of cosine similarity as the dropping metric is provided in Table 4.

Block Drop Transformer models are composed of stacked blocks, where each block shares a common architecture and can be viewed as a subnetwork. To reduce complexity, we first consider dropping entire blocks that are deemed unimportant.

As shown in Figure 2, Transformer blocks operate sequentially, with each block's output feeding into the next. To evaluate redundancy, we compute the similarity between the input and output of each block. For the l-th block, the importance score is calculated as:

$$\boldsymbol{S}_B^l = 1 - \text{CosineSim}(\boldsymbol{X}_B^l, \boldsymbol{Y}_B^l), \tag{2}$$

where $\boldsymbol{X}_B^l$ and $\boldsymbol{Y}_B^l$ denote the input and output of the l-th block, respectively. Since the similarity scores are computed locally, we can offload irrelevant modules to save memory. By iteratively computing the importance scores for each block from shallow to deep, we can identify and drop blocks with the lowest scores, thus saving memory and computational resources.

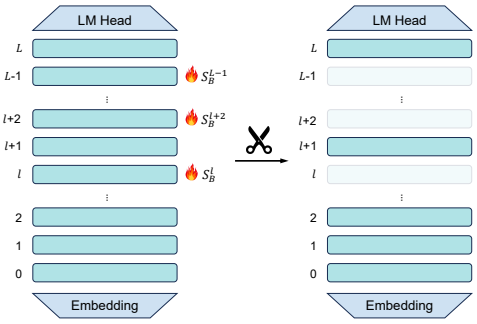

Figure 1: **Visualization of Block Drop**. where we use 🔥 to denote the blocks with high similarity scores. The dropped blocks are blurred.

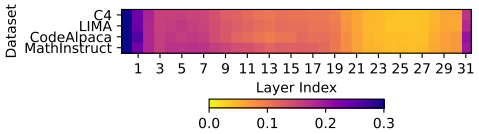

Figure 2: Importance scores of Blocks.

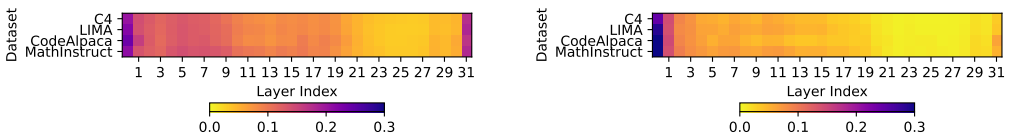

Figure 3: Importance scores for MLP (left) and Attention (right) layers, using various calibration datasets for comprehensive analysis.

3.2 Motivation

Block Drop is an aggressive technique that risks removing essential layers, as it overlooks the internal fine-grained architectures within each block. Given a transformer

block consists of both an Attention layer and an MLP layer. These layers perform distinct functions, with the Attention layer facilitating contextual information flow between tokens and the MLP layer transforming the token representations. Given their distinct roles, we assess the redundancy of each layer separately by measuring the importance scores of Attention and MLP layers individually. Specifically, we leverage multiple calibration datasets to measure the importance scores, ranging from the pretraining dataset (e.g., C4 (Raffel et al., 2020)) to instruction fine-tuning datasets (e.g., CodeAlpaca-20k (Rozière et al., 2024), MathInstruct (Yue et al., 2024) and LIMA (Zhou et al., 2024)). Figure 2 and 3 illustrate the varying trend of importance scores for Attention layers compared to MLP layers across multiple datasets. This observation motivates us to consider the varying levels of redundancy between MLP and Attention layers and to develop more fine-grained dropping techniques accordingly, namely, MLP Drop and Attention Drop.

3.3 Layer Drop.

MLP Drop As illustrated in Figure 4, each MLP layer follows a LayerNorm operation and involves a residual connection, ensuring that part of the input is preserved in the final output. Given the input $\boldsymbol{X}_M^l$ of the LayerNorm before MLP at the l-th Block, the output $\boldsymbol{Y}_M^l$ can be formulated as:

$$\boldsymbol{Y}_M^l = \boldsymbol{X}_M^l + \text{MLP}(\text{LayerNorm}(\boldsymbol{X}_M^l)). \tag{3}$$

Since the output $\boldsymbol{Y}_M^l$ contains both the residual and the MLP transformation, evaluating similarity based solely on the MLP's output can be misleading. To address this, we consider the MLP layer and its associated LayerNorm as a single unit and compute their importance score as follows:

$$\boldsymbol{S}_M^l = 1 - \text{CosineSim}(\boldsymbol{X}_M^l, \boldsymbol{Y}_M^l). \tag{4}$$

By treating these layers as a single entity, we ensure a more accurate measure of importance. MLP Drop removes both the unimportant MLP and associated LayerNorm layers. Further validation of this approach can be found in Appendix C.

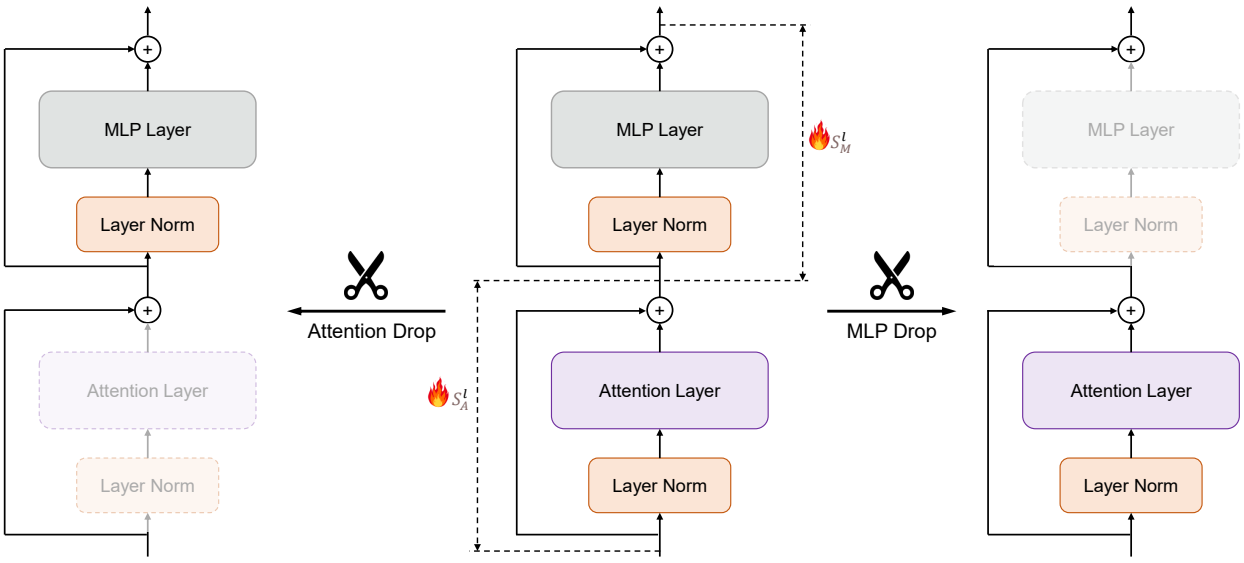

Figure 4: **Visualization of Layer Drop**, where we visualize dropping either MLP or Attention Layers. Given the residual connection, we take LayerNorm together with the corresponding layers. The dropped layers with high similarity scores 🔥 are blurred.

Attention Drop Similarly, Attention layers also operate within a residual connection. The output of the l-th Attention layer is computed as:

$$\boldsymbol{Y}_A^l = \boldsymbol{X}_A^l + \text{Attention}(\text{LayerNorm}(\boldsymbol{X}_A^l)), \tag{5}$$

where $\boldsymbol{X}_A^l$ is the inputs of the corresponding LayerNorm layers and $\boldsymbol{Y}_A^l$ overall outputs that involves residual connections. Like MLP Drop, we assess both the Attention layer and its associated LayerNorm as a single unit. The importance score for the Attention layer is:

$$\boldsymbol{S}_A^l = 1 - \text{CosineSim}(\boldsymbol{X}_A^l, \boldsymbol{Y}_A^l). \tag{6}$$

Layer Drop, for both MLP and Attention layers, is performed in a one-shot manner, calculating importance scores once and removing redundant layers in a single step. This approach avoids the resource-intensive and time-consuming iterative pruning process. The effectiveness of this simple one-shot technique is evaluated in Appendix C.

4 Investigation of Dropping Different Target Modules

In this section, we conduct a comprehensive investigation into the effects of dropping different target modules. To quantify the trade-off between performance degradation and speedup, we introduce a new metric, i.e., **Speedup Degradation Ratio (SDR)**, defined as:

$$\gamma = \frac{\Delta\text{Avg.}}{\Delta\text{Speedup}}, \tag{7}$$

where ΔAvg. represents the percentage change in average performance across the evaluated tasks, and ΔSpeedup denotes the corresponding percentage of speedup achieved by each method. Therefore, γ measures the amount of performance degradation incurred for each 1% increase in speedup. A lower γ value indicates that the model achieves speedup with minimal performance loss, making it more efficient. In contrast, a higher γ value suggests that the performance loss is substantial relative to the speedup gained, implying a less favorable trade-off.

Table 1: **Experimental results of dropping different modules**. We drop a fixed number of modules (e.g., 4 or 8) in the Mistral-7B model. The Block Drop baseline is adapted from ShortGPT (Men et al., 2024). Rows with averaged performance lower than 95% of the original performance are grayed.

Method	ARC-C	BoolQ	HellaSwag	MMLU	OBQA	PIQA	RTE	WinoGrande	Avg. (↑)	SpeedUp (↑)	γ (↓)
Baseline	61.5	83.7	83.2	62.5	43.8	82.0	66.8	78.5	70.3	1.00×	–
Block-4	53.1	80.4	77.5	61.6	40.0	77.6	70.0	76.6	67.1	1.14×	0.23
Block-8	40.0	71.6	63.9	60.0	30.6	69.3	63.9	69.7	58.6	1.32×	0.37
MLP-4	53.2	80.3	77.7	61.7	40.0	77.6	67.5	77.3	66.9	1.03×	1.13
MLP-8	36.7	71.8	33.6	53.3	30.6	68.0	66.8	66.6	53.4	1.06×	2.82
Attn-4	61.0	83.5	82.9	62.5	44.6	82.0	64.6	78.0	69.9	1.10×	0.04
Attn-8	60.2	82.7	82.3	62.2	44.2	81.3	66.8	78.8	69.8	1.23×	0.02
Attn-12	57.2	76.8	80.2	59.4	41.8	79.1	66.1	77.7	67.3	1.40×	0.08

Table 1 and Figure 5 summarize the results of dropping different target modules, such as Block, MLP, and Attention layers. Specifically, Table 1 shows the performance impact of dropping a fixed number of modules (e.g., 4 and 8 layers), while Figure 5 extends this analysis by evaluating a broader range of dropping ratios (0% to 100%).

Cosine Similarity as an Effective Metric for Layer Dropping Building on the implementation details provided in Appendix A, we first compare the effectiveness of various layer dropping metrics against cosine similarity. Specifically, we evaluate the reverse order and relative magnitude metrics proposed by ShortGPT (Men et al., 2024) and apply them to the Attention Drop setting. In addition, we take the random dropping of attention layers as a

Table 2: Comparison of Dropping Metrics. The reported results reflect the average performance across HellaSwag, MMLU, OBQA, and WinoGrande.

Metric	Attn-4	Attn-8	Attn-12
Random	61.5	49.6	39.4
Reverse Order	66.9	66.9	61.5
Relative Magnitude	67.0	66.8	62.3
Cosine Similarity	**67.0**	**66.9**	**64.8**

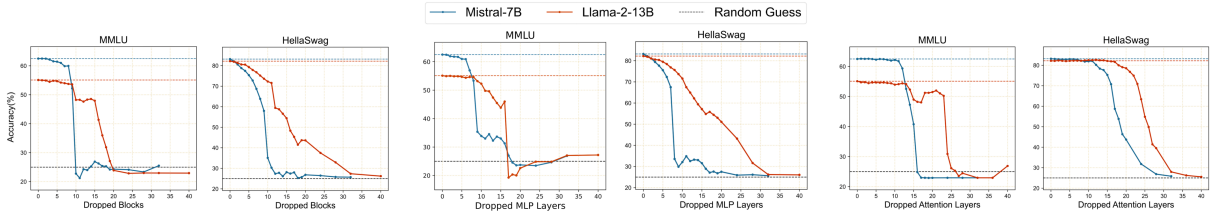

(a) Block Drop (b) MLP Drop (c) Attention Drop

Figure 5: **Performance with respect to Dropping Ratios**. The solid lines represent the impact of dropping the n modules with the lowest importance scores in Mistral-7B and Llama-2-13B, and the dotted lines represent the performances of the baseline and random guessing.

baseline. All experiments were conducted using the Mistral-7B model, with performance averaged over five different random seeds. As shown in Table 2, our proposed metric, Cosine Similarity, consistently outperformed the others and is therefore selected as the default metric for dropping decisions.

Block and MLP Drop: Significant Performance Degradation with Moderate Speedup Block Drop and MLP Drop both lead to notable performance declines across both models, despite achieving moderate speedups. For instance, dropping 8 blocks causes a 11.7% performance drop, which is unacceptable in practice. Similarly, MLP Drop exhibits a comparable trend, with a small decline at 4 layers (3.4%, $\gamma = 1.13$), but a much larger drop at 8 layers (13.5%, $\gamma = 2.82$). **These results suggest that while Block and MLP Drop provide moderate speedup, they do so at the cost of significant performance degradation, especially at higher drop ratios.**

Attention Drop: Minimal Performance Impact with High Efficiency Surprisingly, despite the critical role of attention layers in Transformer architectures, dropping attention layers is highly effective. Mistral-7B maintains over 95% of the original performance even after dropping 12 attention layers with a speedup of 1.40× and a low γ of 0.08, as shown in Table 1. The superior performance of Attention Drop persists when compared to other compression techniques in Appendix C. **These results demonstrate that attention layers are highly redundant, and their removal has minimal impact on model accuracy, making Attention Drop a highly efficient pruning strategy.**

Table 3: Experimental results on Llama-3-8B and Llama-3-70B.

Method	HellaSwag	MMLU	OBQA	WinoGrande	Avg. (↑)	SpeedUp (↑)	γ (↓)
Llama-3-8B							
Baseline	82.2	65.5	45.0	77.7	67.6	1.00×	–
Attn-4	81.6	65.1	44.8	78.2	67.4	1.07×	0.03
Attn-8	81.1	65.1	45.0	78.4	67.4	1.16×	0.01
Attn-12	79.4	63.9	42.2	77.8	65.8	1.26×	0.07
Attn-16	71.2	38.2	39.4	72.8	55.4	1.38×	0.32
Attn-20	42.2	23.0	30.6	58.7	38.6	1.52×	0.56
Llama-3-70B							
Baseline	88.0	78.7	48.4	85.4	75.1	1.00×	–
Attn-4	87.9	78.7	49.0	85.2	75.2	1.04×	-0.03
Attn-8	87.8	78.5	48.8	85.2	75.1	1.10×	0.00
Attn-16	87.8	78.7	48.6	84.9	75.0	1.17×	0.01
Attn-32	87.9	78.6	48.8	85.3	75.2	1.35×	0.00
Attn-40	85.2	77.1	48.0	82.8	73.3	1.43×	0.00
Attn-48	81.2	73.9	47.4	81.3	71.0	1.55×	0.07

To verify the consistency of our Attention Drop findings on larger models, we evaluate LLaMA-3-70B as shown in Table 3, which demonstrates a speedup of 1.55 and a γ of 0.07 when dropping 40 out of 80 attention layers. **This robustness indicates that larger models can also tolerate the removal of a significant proportion of Attention layers without degrading performance.**

Attention Drop achieves substantial speedup with minimal performance degradation and outperforms other mainstream compression methods, as shown in Appendix C. Moreover, given the high redundancy observed in certain MLP layers, we further propose the advanced *Joint Layer Drop* approach, which removes both less important Attention and MLP layers. Additional details of Joint Layer Drop are provided in Appendix B.

5 Efficiency of Attention Drop

In this section, we evaluate the efficiency of Attention Drop in terms of both memory usage and inference speed. Specifically, we examine the reduction in memory overhead due to the key-value (KV) cache and measure the speed-up during the entire generation phase.

KV-cache Memory Reduction Given the auto-regressive nature of attention, where outputs are generated token by token, the KV-cache is used to store intermediate representations of input sequences. This cache helps accelerate inference by preventing redundant computations but comes with a significant memory cost, especially with longer sequence lengths or larger batch sizes. Our proposed Attention Drop method efficiently removes unimportant attention layers, reducing the corresponding KV-cache. Table 4 provides a comparison of 16-bit precision KV-cache memory usage before and after Attention Drop for various models, where we use 8 Nvidia RTX A6000 Ada GPUs for the 70B models and 4 Nvidia RTX A6000 Ada GPUs for other smaller models. As shown, Attention Drop results in substantial memory savings across all tested models. For instance, the KV-cache decreases from 20GB to 10GB in Llama-3-70B. Note the reported results are based on resource-constrained scenarios. In resource-sufficient cases, where larger batch sizes and longer sequence lengths can be applied, the memory usage savings from Attention Drop become even more significant.

Table 4: **Comparison of KV-cache sizes before and after Attention Drop** across different models, with a sequence length of 2048. Since Llama-2-13B does not use grouped-query attention, its KV-cache costs are higher.

Model	Batch Size	wo/Attn Drop		w/Attn Drop	
		Layers	KV-cache	Layers	KV-cache
Mistral-7B	64	32	16GB	20	10GB
Llama-2-13B	32	40	52GB	20	26GB
Llama-2-70B	32	80	20GB	40	10GB
Llama-3-8B	64	32	16GB	20	10GB
Llama-3-70B	32	80	20GB	40	10GB

Speed Measurement We also evaluate the run-time speed improvements achieved through Attention Drop. The inference speed is measured throughout the entire generation process, starting from the input prompt to the generation of the final token. To ensure that the results accurately reflect the speed improvements, we follow two key principles in our setup: (1) all operations are performed on a single Nvidia RTX A6000 Ada GPU, avoiding any communication overhead caused by multi-GPU setups; and (2) we increase the batch sizes to maximize GPU utilization for each model. Specifically, for Llama-3-70B, we employ 4-bit quantization due to its large model size, while noting that Attention Drop is orthogonal to quantization shown in Appendix D. For Llama-3-8B and Mistral-7B, we use 16-bit precision. We use an input sequence of 2048 tokens and autoregressively generate an additional 2048 tokens. This setup allows us to capture the full inference process, ensuring that both the prefill and the decoding stages are included in the speed measurements.

The speed-up ratios achieved through Attention Drop are presented in Tables 1, 3, and 10. Our results show that Attention Drop provides up to 40% speed-up while retaining more than 95% of the original model's performance. Additionally, as demonstrated in Table 1, the γ values for Attention Drop are significantly lower than those for MLP Drop and Block Drop, especially at higher speed-up ratios. This indicates that Attention Drop achieves a more efficient trade-off between speed and performance, making it a superior method for model acceleration.

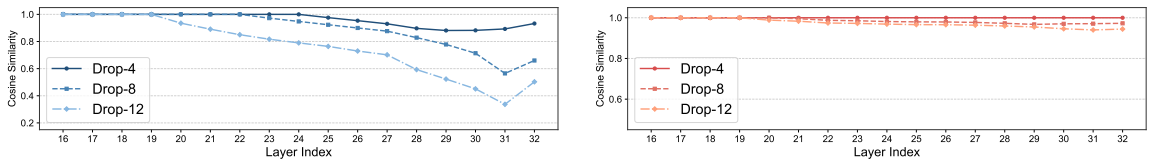

(a) MLP Drop (b) Attention Drop

Figure 6: **Layer-wise cosine similarity** between the output embeddings of the original model and models with varying numbers of dropped **(a) MLP** or **(b) Attention** layers. Since all dropped layers are located in the second half of the network, only the corresponding layers are shown for clarity.

6 Visualization and Analysis of Layer Importance

In this section, we visualize the importance scores and the corresponding dropping order of pretrained models. We then trace back through historical checkpoints to explore the dynamics of importance scores throughout the training process.

6.1 Impact of Layer Drop on Embedding Representations

We have demonstrated the effectiveness of using layer-wise cosine similarity in the middle layers to guide layer dropping. We now examine how layer dropping alters the embeddings of the original model. Specifically, we extract the output embeddings of each layer from both the original and compressed models and compute the cosine similarity between them. As shown in Figure 6, dropping MLP layers leads to substantial fluctuations in the embeddings, whereas dropping attention layers maintains a high degree of similarity with the original model. The low similarity observed in the model with MLP dropping results in a significant divergence in the predicted tokens and failure to produce the correct answer, as illustrated in Figure 7. In contrast, both the original model and the model with 12 dropped attention layers are able to generate the correct answer. These findings align with the observation that MLP layers are primarily responsible for storing knowledge (Geva et al., 2021; Gromov et al., 2024).

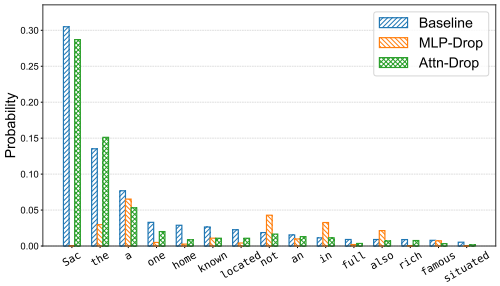

Figure 7: **Output token probability distributions** of models before and after dropping 12 layers. The input query is "The capital of California is".

On the other hand, since MLP layers perform token transformations in high-dimensional space, MLP dropping directly impacts the model's sensitivity to different tokens. Since the embedding of the last token depends on both itself and its preceding context, we switch the last token and monitor the resulting embedding from different forwarding passes. As shown in Figure 8, the original model exhibits low similarity across different inputs, which is consistent with the generative diversity of language models, where varying the current token leads to different subsequent tokens. In contrast, models with MLP dropping lack this capability and produce highly similar embeddings for different input tokens. This suggests that such models lose the ability to distinguish between different tokens, resulting in degraded performance. Meanwhile, models with attention dropping exhibit trends comparable to those of the original model, indicating the presence of less impactful attention layers, which we further investigate in the following sections.

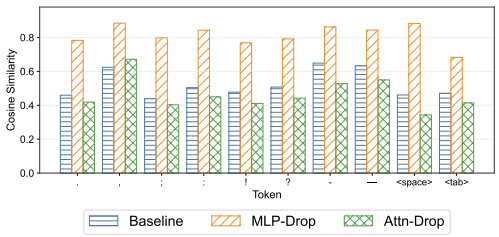

Figure 8: **Cosine similarity of the last-token embedding** before and after replacing the last token with different candidates, given the input query: "In mammals, the diaphragm is the primary muscle responsible for the act of _____".

6.2 Deeper Modules with Higher Redundancy

Based on Figure 2, 3 and 16, we observe that the deeper layers (excluding the last ones) often exhibit excessively low importance across Block, MLP, and Attention modules.

To further analyze the dropped modules, we visualize the dropped layers or blocks with different dropping ratios. Figure 9 visualizes the remaining and dropped layers/blocks as the number of dropped modules increases. Llama-2-13B and Mistral-7B exhibit similar patterns in Layer Drop and Block Drop: initially, both models tend to drop the deeper layers, followed by the shallower ones. These findings are consistent with Men et al. (2024), which suggests that deeper layers tend to be more redundant. Larger models (e.g., Llama-2-70B) also showcase a similar trend in Appendix D.

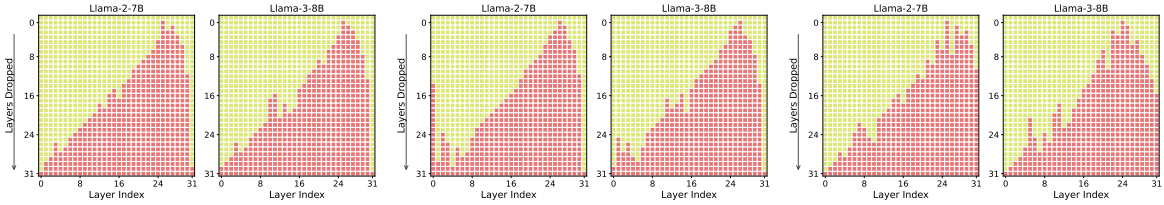

(a) Block Drop (b) MLP Drop (c) Attention Drop

Figure 9: **Visualization of Dropping Order**, where each row represents the corresponding retained and dropped layers/blocks for a specific number of dropped layers/blocks.

Previous studies on layer analysis in neural networks (Dalvi et al., 2022; Sajjad et al., 2022) have demonstrated that shallow layers are more important than deeper layers, since they primarily model local word interactions, which are critical for capturing morphology and lexical semantics. These layers provide essential input to the higher layers, and their removal can therefore be catastrophic. Building on this, we further investigate the differing behaviors of shallow and deep attention layers. Figure 10 compares the attention score matrices of a shallow layer and a deep layer. The shallow layer effectively captures relationships between tokens, whereas the deep layer exhibits a sparse pattern, with attention concentrated along the diagonal and in specific columns.

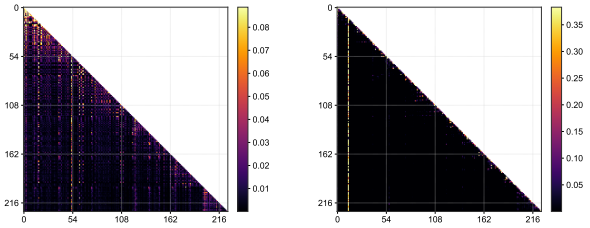

(a) 4th Layer (b) 25th Layer

Figure 10: Attention scores in the shallow layer and deep layer.

6.3 Consistent Redundancy of Attention Layers Throughout Training

Now that the deep layers exhibit high redundancy, to investigate how such a pattern is achieved, we revisit the historical checkpoints to track the dynamic changing of layer-wise importance scores.

Specifically, we use checkpoints released by MAP-Neo-7B (Zhang et al., 2024), since it released continuous checkpoints during training stages. Figure 11 presents the importance scores of Blocks and Layers at different training stages, where Attention layers demonstrate consistently lower importance scores than MLP and Block at all training stages. While the importance scores for MLP layers and Blocks gradually increase as training progresses, the importance scores of Attention layers change much more slowly, consistently exhibiting low importance throughout the training process.

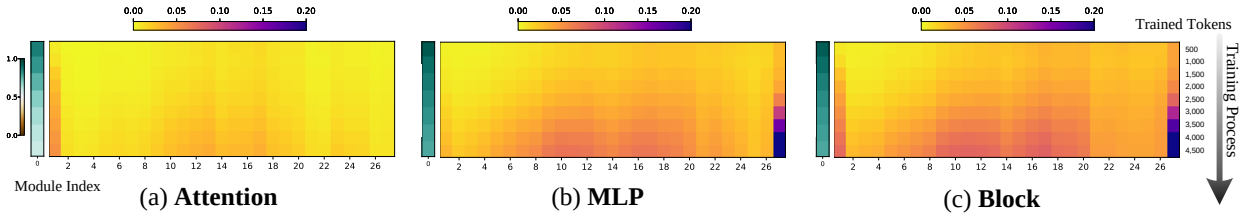

(a) **Attention** (b) **MLP** (c) **Block**

Figure 11: **Visualization of Importance Scores in Checkpoints during the Pre-training Process of MAP-Neo-7B**, where lighter areas represent low importance scores (i.e., high similarity scores). We present the entire Training Process (checkpoints for every 500B trained tokens). We independently visualize the importance scores at the module index 0, since they are significantly higher.
In addition, since randomly initialized models prior to training also exhibit low importance in certain attention layers (as shown in Figure 19), we attribute this phenomenon to intrinsic properties of the attention mechanism, which can be formulated as a weighted linear combination:

$$\boldsymbol{Y}_i = \left(\sum_{j=1}^{i} A_{ij} \boldsymbol{X}_j W_V \right) W_O = \sum_{j=1}^{i} A_{ij} \left(\boldsymbol{X}_j W_V W_O \right), \quad A = \text{softmax}\left(\frac{(\boldsymbol{X}W_Q)(\boldsymbol{X}W_K)^\top}{\sqrt{d_k}} \right), \tag{8}$$

where $\boldsymbol{Y}_i$ denotes the output of the i-th token, which depends on the first i tokens. However, as shown by the attention sinks in Figure 10, attention disproportionately focuses on early tokens (e.g., the t-th token), causing the term $A_{it}\boldsymbol{X}_t$ to dominate the sum $\sum_{j=1}^{i} A_{ij}\boldsymbol{X}_j$. This sparse localized focus effectively limits the contribution of the attention branch to the residual connections.

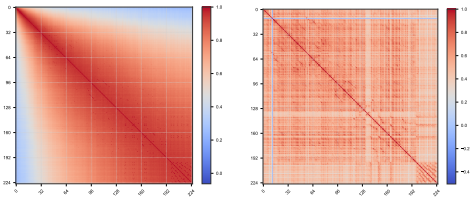

(a) Randomly Init. (b) Pretrained

Figure 12: Token-to-token similarity in deep layers, with the complete visualization in Appendix A.

On the other hand, Attention also has the potential to increase similarity between neighboring tokens, e.g., both the i-th token and i-th aggregate the first i tokens. Through progressively aggregation in multiple layers, even distant tokens can maintain a high degree of similarity, as shown in Figure 12. Notably, the high token-to-token similarity observed in a randomly initialized model further highlights the inherent aggregation behavior of the attention mechanism. More detailed visualizations and analyses are provided in Appendix A.

Consequently, such high similarity between tokens (i.e., over-smoothed tokens Wu et al. (2023)) limits the degree of representational updates in attention layers, since aggregating nearly identical tokens has a diminished effect on the hidden states. Moreover, due to the sparse patterns of attention weights and the low magnitude of the attention branch, as shown in Figure 13, the updates from the attention layers are further constrained. This limitation diminishes the functional contribution of certain attention layers, thereby reducing their relative importance within the model.

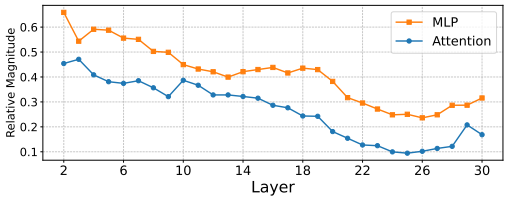

Figure 13: Relative magnitude of layer outputs compared to the residual branch.

7 Discussions and Conclusion

Insights for Future Network Architecture Design Despite the success of scaling up LLMs, our work provides valuable insights for scaling down models to achieve more efficient architectures. One key insight is the high redundancy in attention layers, particularly in deeper layers, which suggests that future works could reduce the number of attention layers without sacrificing performance, rather than maintaining parity with MLP layers. Moreover, unlike MLP layers, attention layers exhibit consistent redundancy as training progresses. This consistency may pose a bottleneck in training large models. To address this, future research could explore replacing attention layers with alternative mechanisms or develop new training techniques that capitalize on this redundancy to further enhance language model capacity.

Limitations While our proposed dropping techniques improve efficiency in the models we evaluated, there are limitations. A key area for future work is testing the applicability of these techniques across a broader range of models, such as vision transformers and vision-language models. Furthermore, our methods focus on post-training dropping without involving retraining, which could potentially recover or even improve performance after pruning as illustrated in Appendix D. Retraining these models could unlock even greater efficiency in more compact architectures.

Conclusion In this work, we systematically revisited transformer architectures by investigating the effects of dropping three types of structures: Blocks, MLP layers, and Attention layers. Our findings reveal that attention layers display significant redundancy and can be removed in large proportions without compromising performance. To build on this, we introduced Joint Layer Drop, a method that further increases both dropping ratios and performance by targeting redundant layers across both MLP and Attention layers. This study empirically demonstrates the potential for creating more compact and efficient transformer models, providing valuable insights for future network design within the NLP community. By exploring structured redundancy, we open up new avenues for designing more efficient, scalable models that maintain high performance even under resource constraints.

References

Winogrande: An adversarial winograd schema challenge at scale. 2019.

Yonatan Bisk, Rowan Zellers, Ronan Le Bras, Jianfeng Gao, and Yejin Choi. Piqa: Reasoning about physical commonsense in natural language, 2019.

Iñigo Casanueva, Tadas Temčinas, Daniela Gerz, Matthew Henderson, and Ivan Vulić. Efficient intent detection with dual sentence encoders. *arXiv preprint arXiv:2003.04807*, 2020.

Xiaodong Chen, Yuxuan Hu, and Jing Zhang. Compressing large language models by streamlining the unimportant layer. *arXiv preprint arXiv:2403.19135*, 2024.

Wei-Lin Chiang, Zhuohan Li, Zi Lin, Ying Sheng, Zhanghao Wu, Hao Zhang, Lianmin Zheng, Siyuan Zhuang, Yonghao Zhuang, Joseph E. Gonzalez, Ion Stoica, and Eric P. Xing. Vicuna: An open-source chatbot impressing gpt-4 with 90%* chatgpt quality, March 2023. URL https://lmsys.org/blog/2023-03-30-vicuna/.

Christopher Clark, Kenton Lee, Ming-Wei Chang, Tom Kwiatkowski, Michael Collins, and Kristina Toutanova. Boolq: Exploring the surprising difficulty of natural yes/no questions, 2019.

Peter Clark, Isaac Cowhey, Oren Etzioni, Tushar Khot, Ashish Sabharwal, Carissa Schoenick, and Oyvind Tafjord. Think you have solved question answering? try arc, the ai2 reasoning challenge, 2018.

Fahim Dalvi, Abdul Rafae Khan, Firoj Alam, Nadir Durrani, Jia Xu, and Hassan Sajjad. Discovering latent concepts learned in BERT. In *International Conference on Learning Representations*, 2022. URL https://openreview.net/forum?id=POTMtpYI1xH.

Elias Frantar and Dan Alistarh. Sparsegpt: Massive language models can be accurately pruned in one-shot, 2023.

Elias Frantar, Saleh Ashkboos, Torsten Hoefler, and Dan Alistarh. Gptq: Accurate post-training quantization for generative pre-trained transformers, 2023.

Leo Gao, Stella Biderman, Sid Black, Laurence Golding, Travis Hoppe, Charles Foster, Jason Phang, Horace He, Anish Thite, Noa Nabeshima, Shawn Presser, and Connor Leahy. The pile: An 800gb dataset of diverse text for language modeling, 2020.

Leo Gao, Jonathan Tow, Baber Abbasi, Stella Biderman, Sid Black, Anthony DiPofi, Charles Foster, Laurence Golding, Jeffrey Hsu, Alain Le Noac'h, Haonan Li, Kyle McDonell, Niklas Muennighoff, Chris Ociepa, Jason Phang, Laria Reynolds, Hailey Schoelkopf, Aviya Skowron, Lintang Sutawika, Eric Tang, Anish Thite, Ben Wang, Kevin Wang, and Andy Zou. A framework for few-shot language model evaluation, 12 2023. URL https://zenodo.org/records/10256836.

Mor Geva, Roei Schuster, Jonathan Berant, and Omer Levy. Transformer feed-forward layers are key-value memories. In Marie-Francine Moens, Xuanjing Huang, Lucia Specia, and Scott Wen-tau Yih (eds.), *Proceedings of the 2021 Conference on Empirical Methods in Natural Language Processing*, pp. 5484–5495, Online and Punta Cana, Dominican Republic, November 2021. Association for Computational Linguistics. doi: 10.18653/v1/2021.emnlp-main.446. URL https://aclanthology.org/2021.emnlp-main.446/.

Andrey Gromov, Kushal Tirumala, Hassan Shapourian, Paolo Glorioso, and Daniel A. Roberts. The unreasonable ineffectiveness of the deeper layers, 2024.

Albert Gu and Tri Dao. Mamba: Linear-time sequence modeling with selective state spaces, 2024.

Dan Hendrycks, Collin Burns, Steven Basart, Andy Zou, Mantas Mazeika, Dawn Song, and Jacob Steinhardt. Measuring massive multitask language understanding, 2021.

Albert Q. Jiang, Alexandre Sablayrolles, Arthur Mensch, Chris Bamford, Devendra Singh Chaplot, Diego de las Casas, Florian Bressand, Gianna Lengyel, Guillaume Lample, Lucile Saulnier, Lélio Renard Lavaud, Marie-Anne Lachaux, Pierre Stock, Teven Le Scao, Thibaut Lavril, Thomas Wang, Timothée Lacroix, and William El Sayed. Mistral 7b, 2023.

Bo-Kyeong Kim, Geonmin Kim, Tae-Ho Kim, Thibault Castells, Shinkook Choi, Junho Shin, and Hyoung-Kyu Song. Shortened llama: A simple depth pruning for large language models. *ICLR Workshop on Mathematical and Empirical Understanding of Foundation Models (ME-FoMo)*, 2024. URL https://openreview.net/forum?id=18VGxuOdpu.

Jeonghoon Kim, Byeongchan Lee, Cheonbok Park, Yeontaek Oh, Beomjun Kim, Taehwan Yoo, Seongjin Shin, Dongyoon Han, Jinwoo Shin, and Kang Min Yoo. Peri-LN: Revisiting normalization layer in the transformer architecture. In *Forty-second International Conference on Machine Learning*, 2025. URL https://openreview.net/forum?id=ci1S6wmXfO.

Aditya Kusupati, Vivek Ramanujan, Raghav Somani, Mitchell Wortsman, Prateek Jain, Sham Kakade, and Ali Farhadi. Soft threshold weight reparameterization for learnable sparsity. In *Proceedings of the International Conference on Machine Learning*, July 2020.

Se Jung Kwon, Dongsoo Lee, Byeongwook Kim, Parichay Kapoor, Baeseong Park, and Gu-Yeon Wei. Structured compression by weight encryption for unstructured pruning and quantization. In *2020 IEEE/CVF Conference on Computer Vision and Pattern Recognition (CVPR)*, pp. 1906–1915, 2020. doi: 10.1109/CVPR42600.2020.00198.

Rui Li, Jianlin Su, Chenxi Duan, and Shunyi Zheng. Linear attention mechanism: An efficient attention for semantic segmentation, 2020.

Tianle Li, Ge Zhang, Quy Duc Do, Xiang Yue, and Wenhu Chen. Long-context llms struggle with long in-context learning. *arXiv preprint arXiv:2404.02060*, 2024.

Ji Lin, Jiaming Tang, Haotian Tang, Shang Yang, Wei-Ming Chen, Wei-Chen Wang, Guangxuan Xiao, Xingyu Dang, Chuang Gan, and Song Han. Awq: Activation-aware weight quantization for llm compression and acceleration. In *MLSys*, 2024.

Hanxiao Liu, Zihang Dai, David R. So, and Quoc V. Le. Pay attention to mlps, 2021.

Florian Mai, Arnaud Pannatier, Fabio Fehr, Haolin Chen, Francois Marelli, Francois Fleuret, and James Henderson. HyperMixer: An MLP-based Green AI Alternative to Transformers. *arXiv preprint arXiv:2203.03691*, 2022.

Xin Men, Mingyu Xu, Qingyu Zhang, Bingning Wang, Hongyu Lin, Yaojie Lu, Xianpei Han, and Weipeng Chen. Shortgpt: Layers in large language models are more redundant than you expect, 2024.

Todor Mihaylov, Peter Clark, Tushar Khot, and Ashish Sabharwal. Can a suit of armor conduct electricity? a new dataset for open book question answering, 2018.

OpenAI. Gpt-4 technical report, 2024.

Baolin Peng, Chunyuan Li, Pengcheng He, Michel Galley, and Jianfeng Gao. Instruction tuning with gpt-4. *arXiv preprint arXiv:2304.03277*, 2023a.

Bo Peng, Eric Alcaide, Quentin Anthony, Alon Albalak, Samuel Arcadinho, Stella Biderman, Huanqi Cao, Xin Cheng, Michael Chung, Matteo Grella, Kranthi Kiran GV, Xuzheng He, Haowen Hou, Jiaju Lin, Przemyslaw Kazienko, Jan Kocon, Jiaming Kong, Bartlomiej Koptyra, Hayden Lau, Krishna Sri Ipsit Mantri, Ferdinand Mom, Atsushi Saito, Guangyu Song, Xiangru Tang, Bolun Wang, Johan S. Wind, Stanislaw Wozniak, Ruichong Zhang, Zhenyuan Zhang, Qihang Zhao, Peng Zhou, Qinghua Zhou, Jian Zhu, and Rui-Jie Zhu. Rwkv: Reinventing rnns for the transformer era, 2023b.

Reiner Pope, Sholto Douglas, Aakanksha Chowdhery, Jacob Devlin, James Bradbury, Anselm Levskaya, Jonathan Heek, Kefan Xiao, Shivani Agrawal, and Jeff Dean. Efficiently scaling transformer inference, 2022.

Colin Raffel, Noam Shazeer, Adam Roberts, Katherine Lee, Sharan Narang, Michael Matena, Yanqi Zhou, Wei Li, and Peter J. Liu. Exploring the limits of transfer learning with a unified text-to-text transformer. *arXiv e-prints*, 2019.

Colin Raffel, Noam Shazeer, Adam Roberts, Katherine Lee, Sharan Narang, Michael Matena, Yanqi Zhou, Wei Li, and Peter J Liu. Exploring the limits of transfer learning with a unified text-to-text transformer. *Journal of machine learning research*, 21(140):1–67, 2020.

Baptiste Rozière, Jonas Gehring, Fabian Gloeckle, Sten Sootla, Itai Gat, Xiaoqing Ellen Tan, Yossi Adi, Jingyu Liu, Romain Sauvestre, Tal Remez, Jérémy Rapin, Artyom Kozhevnikov, Ivan Evtimov, Joanna Bitton, Manish Bhatt, Cristian Canton Ferrer, Aaron Grattafiori, Wenhan Xiong, Alexandre Défossez, Jade Copet, Faisal Azhar, Hugo Touvron, Louis Martin, Nicolas Usunier, Thomas Scialom, and Gabriel Synnaeve. Code llama: Open foundation models for code, 2024. URL https://arxiv.org/abs/2308.12950.

Hassan Sajjad, Nadir Durrani, Fahim Dalvi, Firoj Alam, Abdul Khan, and Jia Xu. Analyzing encoded concepts in transformer language models. In Marine Carpuat, Marie-Catherine de Marneffe, and Ivan Vladimir Meza Ruiz (eds.), *Proceedings of the 2022 Conference of the North American Chapter of the Association for Computational Linguistics: Human Language Technologies*, pp. 3082–3101, Seattle, United States, July 2022. Association for Computational Linguistics. doi: 10.18653/v1/2022.naacl-main.225. URL https://aclanthology.org/2022.naacl-main.225/.

Victor Sanh, Thomas Wolf, and Alexander M. Rush. Movement pruning: Adaptive sparsity by fine-tuning, 2020. URL https://arxiv.org/abs/2005.07683.

Dachuan Shi, Chaofan Tao, Ying Jin, Zhendong Yang, Chun Yuan, and Jiaqi Wang. UPop: Unified and progressive pruning for compressing vision-language transformers. In *Proceedings of the 40th International Conference on Machine Learning*, volume 202, pp. 31292–31311. PMLR, 2023.

Mingjie Sun, Zhuang Liu, Anna Bair, and J. Zico Kolter. A simple and effective pruning approach for large language models. *arXiv preprint arXiv:2306.11695*, 2023.

Gemini Team. Gemini 1.5: Unlocking multimodal understanding across millions of tokens of context, 2024.

Gemma Team, Aishwarya Kamath, Johan Ferret, Shreya Pathak, Nino Vieillard, Ramona Merhej, Sarah Perrin, Tatiana Matejovicova, Alexandre Ramé, Morgane Rivière, Louis Rouillard, Thomas Mesnard, Geoffrey Cideron, Jean bastien Grill, Sabela Ramos, Edouard Yvinec, Michelle Casbon, Etienne Pot, Ivo Penchev, Gaël Liu, Francesco Visin, Kathleen Kenealy, Lucas Beyer, Xiaohai Zhai, Anton Tsitsulin, Robert Busa-Fekete, Alex Feng, Noveen Sachdeva, Benjamin Coleman, Yi Gao, Basil Mustafa, Iain Barr, Emilio Parisotto, David Tian, Matan Eyal, Colin Cherry, Jan-Thorsten Peter, Danila Sinopalnikov, Surya Bhupatiraju, Rishabh Agarwal, Mehran Kazemi, Dan Malkin, Ravin Kumar, David Vilar, Idan Brusilovsky, Jiaming Luo, Andreas Steiner, Abe Friesen, Abhanshu Sharma, Abheesht Sharma, Adi Mayrav Gilady, Adrian Goedeckemeyer, Alaa Saade, Alex Feng, Alexander Kolesnikov, Alexei Bendebury, Alvin Abdagic, Amit Vadi, András György, André Susano Pinto, Anil Das, Ankur Bapna, Antoine Miech, Antoine Yang, Antonia Paterson, Ashish Shenoy, Ayan Chakrabarti, Bilal Piot, Bo Wu, Bobak Shahriari, Bryce Petrini, Charlie Chen, Charline Le Lan, Christopher A. Choquette-Choo, CJ Carey, Cormac Brick, Daniel Deutsch, Danielle Eisenbud, Dee Cattle, Derek Cheng, Dimitris Paparas, Divyashree Shivakumar Sreepathihalli, Doug Reid, Dustin Tran, Dustin Zelle, Eric Noland, Erwin Huizenga, Eugene Kharitonov, Frederick Liu, Gagik Amirkhanyan, Glenn Cameron, Hadi Hashemi, Hanna Klimczak-Plucińska, Harman Singh, Harsh Mehta, Harshal Tushar Lehri, Hussein Hazimeh, Ian Ballantyne, Idan Szpektor, Ivan Nardini, Jean Pouget-Abadie, Jetha Chan, Joe Stanton, John Wieting, Jonathan Lai, Jordi Orbay, Joseph Fernandez, Josh Newlan, Ju yeong Ji, Jyotinder Singh, Kat Black, Kathy Yu, Kevin Hui, Kiran Vodrahalli, Klaus Greff, Linhai Qiu, Marcella Valentine, Marina Coelho, Marvin Ritter, Matt Hoffman, Matthew Watson, Mayank Chaturvedi, Michael Moynihan, Min Ma, Nabila Babar, Natasha Noy, Nathan Byrd, Nick Roy, Nikola Momchev, Nilay Chauhan, Noveen Sachdeva, Oskar Bunyan, Pankil Botarda, Paul Caron, Paul Kishan Rubenstein, Phil Culliton, Philipp Schmid, Pier Giuseppe Sessa, Pingmei Xu, Piotr Stanczyk, Pouya Tafti, Rakesh Shivanna, Renjie Wu, Renke Pan, Reza Rokni, Rob Willoughby, Rohith Vallu, Ryan Mullins, Sammy Jerome, Sara Smoot, Sertan Girgin, Shariq Iqbal, Shashir Reddy, Shruti Sheth, Siim Põder, Sijal Bhatnagar, Sindhu Raghuram Panyam, Sivan Eiger, Susan Zhang, Tianqi Liu, Trevor Yacovone, Tyler Liechty, Uday Kalra, Utku Evci, Vedant Misra, Vincent Roseberry, Vlad Feinberg, Vlad Kolesnikov, Woohyun Han, Woosuk Kwon, Xi Chen, Yinlam Chow, Yuvein Zhu, Zichuan Wei, Zoltan Egyed, Victor Cotruta, Minh Giang, Phoebe Kirk, Anand Rao, Kat Black, Nabila Babar, Jessica Lo, Erica Moreira, Luiz Gustavo

Martins, Omar Sanseviero, Lucas Gonzalez, Zach Gleicher, Tris Warkentin, Vahab Mirrokni, Evan Senter, Eli Collins, Joelle Barral, Zoubin Ghahramani, Raia Hadsell, Yossi Matias, D. Sculley, Slav Petrov, Noah Fiedel, Noam Shazeer, Oriol Vinyals, Jeff Dean, Demis Hassabis, Koray Kavukcuoglu, Clement Farabet, Elena Buchatskaya, Jean-Baptiste Alayrac, Rohan Anil, Dmitry, Lepikhin, Sebastian Borgeaud, Olivier Bachem, Armand Joulin, Alek Andreev, Cassidy Hardin, Robert Dadashi, and Léonard Hussenot. Gemma 3 technical report, 2025. URL https://arxiv.org/abs/2503.19786.

Hugo Touvron, Thibaut Lavril, Gautier Izacard, Xavier Martinet, Marie-Anne Lachaux, Timothée Lacroix, Baptiste Rozière, Naman Goyal, Eric Hambro, Faisal Azhar, Aurelien Rodriguez, Armand Joulin, Edouard Grave, and Guillaume Lample. Llama: Open and efficient foundation language models, 2023.

Ashish Vaswani. Attention is all you need. *arXiv preprint arXiv:1706.03762*, 2017.

Alex Wang, Amanpreet Singh, Julian Michael, Felix Hill, Omer Levy, and Samuel R. Bowman. GLUE: A multi-task benchmark and analysis platform for natural language understanding. 2019. In the Proceedings of ICLR.

Tiannan Wang, Wangchunshu Zhou, Yan Zeng, and Xinsong Zhang. EfficientVLM: Fast and accurate vision-language models via knowledge distillation and modal-adaptive pruning. In Anna Rogers, Jordan Boyd-Graber, and Naoaki Okazaki (eds.), *Findings of the Association for Computational Linguistics: ACL 2023*, pp. 13899–13913, Toronto, Canada, July 2023. Association for Computational Linguistics. doi: 10.18653/v1/2023.findings-acl.873. URL https://aclanthology.org/2023.findings-acl.873.

Xinyi Wu, Amir Ajorlou, Zihui Wu, and Ali Jadbabaie. Demystifying oversmoothing in attention-based graph neural networks. In *Thirty-seventh Conference on Neural Information Processing Systems*, 2023. URL https://openreview.net/forum?id=Kg65qieiuB.

Guangxuan Xiao, Yuandong Tian, Beidi Chen, Song Han, and Mike Lewis. Efficient streaming language models with attention sinks. In *The Twelfth International Conference on Learning Representations*, 2024. URL https://openreview.net/forum?id=NG7sS51zVF.

Longhui Yu, Weisen Jiang, Han Shi, Jincheng Yu, Zhengying Liu, Yu Zhang, James T Kwok, Zhenguo Li, Adrian Weller, and Weiyang Liu. Metamath: Bootstrap your own mathematical questions for large language models. *arXiv preprint arXiv:2309.12284*, 2023.

Xiang Yue, Xingwei Qu, Ge Zhang, Yao Fu, Wenhao Huang, Huan Sun, Yu Su, and Wenhu Chen. MAmmoTH: Building math generalist models through hybrid instruction tuning. In *The Twelfth International Conference on Learning Representations*, 2024. URL https://openreview.net/forum?id=yLClGs770I.

Rowan Zellers, Ari Holtzman, Yonatan Bisk, Ali Farhadi, and Yejin Choi. Hellaswag: Can a machine really finish your sentence?, 2019.

Ge Zhang, Scott Qu, Jiaheng Liu, Chenchen Zhang, Chenghua Lin, Chou Leuang Yu, Danny Pan, Esther Cheng, Jie Liu, Qunshu Lin, Raven Yuan, Tuney Zheng, Wei Pang, Xinrun Du, Yiming Liang, Yinghao Ma, Yizhi Li, Ziyang Ma, Bill Lin, Emmanouil Benetos, Huan Yang, Junting Zhou, Kaijing Ma, Minghao Liu, Morry Niu, Noah Wang, Quehry Que, Ruibo Liu, Sine Liu, Shawn Guo, Soren Gao, Wangchunshu Zhou, Xinyue Zhang, Yizhi Zhou, Yubo Wang, Yuelin Bai, Yuhan Zhang, Yuxiang Zhang, Zenith Wang, Zhenzhu Yang, Zijian Zhao, Jiajun Zhang, Wanli Ouyang, Wenhao Huang, and Wenhu Chen. Map-neo: Highly capable and transparent bilingual large language model series, 2024.

Zhenyu Zhang, Ying Sheng, Tianyi Zhou, Tianlong Chen, Lianmin Zheng, Ruisi Cai, Zhao Song, Yuandong Tian, Christopher Ré, Clark Barrett, Zhangyang Wang, and Beidi Chen. H_2o: Heavy-hitter oracle for efficient generative inference of large language models, 2023.

Chunting Zhou, Pengfei Liu, Puxin Xu, Srinivasan Iyer, Jiao Sun, Yuning Mao, Xuezhe Ma, Avia Efrat, Ping Yu, Lili Yu, et al. Lima: Less is more for alignment. *Advances in Neural Information Processing Systems*, 36, 2024.

Tao Zhuang, Zhixuan Zhang, Yuheng Huang, Xiaoyi Zeng, Kai Shuang, and Xiang Li. Neuron-level structured pruning using polarization regularizer. In H. Larochelle, M. Ranzato, R. Hadsell, M.F. Balcan, and H. Lin (eds.), *Advances in Neural Information Processing Systems*, volume 33, pp. 9865–9877. Curran Associates, Inc., 2020. URL https://proceedings.neurips.cc/paper_files/paper/2020/file/703957b6dd9e3a7980e040bee50ded65-Paper.pdf.

A Implementation Details

Models We utilize Llama-2 (Touvron et al., 2023) and Mistral (Jiang et al., 2023) as the default models, given their competitive performance and wide usage. We also evaluated the completely open-source model MAP-Neo (Zhang et al., 2024) to explore the redundancy variations in the modules of the entire pre-training phase. Additionally, we experimented with the newly released Llama-3 to verify the effectiveness of model dropping on the latest models.

Datasets For the calibration dataset, we used the validation set of C4 dataset (Raffel et al., 2019), with 256 samples and an input sequence length of 2,048, following the setup in (Sun et al., 2023). The setting is well-supported by Appendix C. To evaluate model performance, we report normalized zero-shot or few-shot accuracy on the LM-harness benchmark, which includes multiple tasks: ARC-C (Clark et al., 2018), BoolQ (Clark et al., 2019), HellaSwag (Zellers et al., 2019), MMLU (Hendrycks et al., 2021), OBQA (Mihaylov et al., 2018), PIQA (Bisk et al., 2019), RTE (Wang et al., 2019), and WinoGrande (ai2, 2019). Please refer to Table 5 for detailed information. The evaluation code is based on EleutherAI LM Harness (Gao et al., 2023).

Table 5: **Experimental settings for evaluation tasks.** "Norm" refers to the normalization performed with respect to the length of the input.

Task	Number of few-shot	Metric
BoolQ	0	Accuracy
RTE	0	Accuracy
OBQA	0	Accuracy (Norm)
PIQA	0	Accuracy (Norm)
MMLU	5	Accuracy
WinoGrande	5	Accuracy
GSM8K	5	Exact Match
HellaSwag	10	Accuracy (Norm)
ARC-C	25	Accuracy (Norm)

B Joint Layer Drop Further Enhances the Performance

While a significant proportion of attention layers exhibit high redundancy, our findings also show that some MLP layers have low importance. To further optimize model efficiency, we introduce Joint Layer Drop, which combines both Attention Drop and MLP Drop strategies. This approach leverages the redundancy in both attention and MLP layers to enhance the overall performance of the model.

Methodology: Combining Attention and MLP Drop The Joint Layer Drop method is implemented by first calculating the importance scores for both attention layers ($\boldsymbol{S}_A^l$) and MLP layers ($\boldsymbol{S}_M^l$) individually. By dropping both MLP and attention layers based on the combined set of scores, $\boldsymbol{S} = [\boldsymbol{S}_{\mathrm{A}}^l, \boldsymbol{S}_{\mathrm{M}}^l]$, this joint approach simultaneously removes the most redundant components from both layer types, thereby enhancing model efficiency while preserving performance.

Superior Performance with Joint Layer Drop As demonstrated in Figure 14, Joint Layer Drop consistently achieves better performance than either Attention Drop or MLP Drop alone. The process begins by exclusively dropping attention layers. However, as the dropping ratio increases and the more redundant attention layers are pruned, MLP layers start to become the next most redundant components. At this point, Joint Layer Drop begins to remove MLP layers, leading to further reductions in redundant layers without significant performance loss, e.g., after dropping 31 layers (Attention + MLP), Llama-2-13B still retains 90% of the performance on the MMLU task.

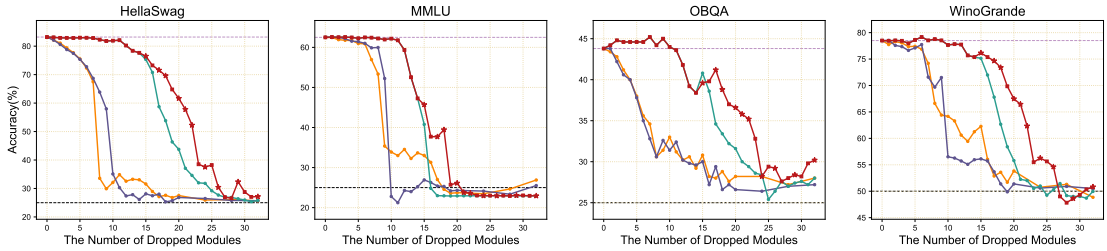

Figure 14: **Accuracy Curves of Dropping Different Target Modules**, where we consider dropping single types of modules and Joint dropping (Attn + MLP). In the line of Joint Drop, ★ represents the step where the MLP is dropped, while the ■ represents the step where the Attention is dropped.

C Ablation Studies

One-Shot v.s. Iterative One-shot and iterative approaches are the two most common methods for model compression. In the one-shot approach, importance scores are computed once, and the model is pruned in a single step. In contrast, the iterative method computes importance scores and prunes the model incrementally over multiple iterations. In Figure 15, we empirically compare Iterative Dropping and One-Shot Dropping, where in Iterative Dropping, layers are removed one by one in each iteration.

As shown in Figure 15, Iterative Dropping achieves performance that is merely comparable to One-Shot Dropping, without offering any significant enhancement. This occurs because removing a layer lowers the similarity scores of deeper layers, making them more critical. As a result, subsequent dropping steps increasingly target shallower layers, accelerating the model's collapse. Given the simplicity and efficiency, One-Shot Dropping emerges as the superior choice.

Residual Connection The involvement of the residual connection ensures a more accurate estimation by accounting for the overall inputs and outputs. To explore its impact on performance, we also consider dropping modules without involving the residual connection. In this case, the importance scores are measured solely by the inputs and outputs of the Attention or MLP layers. As shown in Table 6, the involvement of the residual connection is essential for Layer Drop.

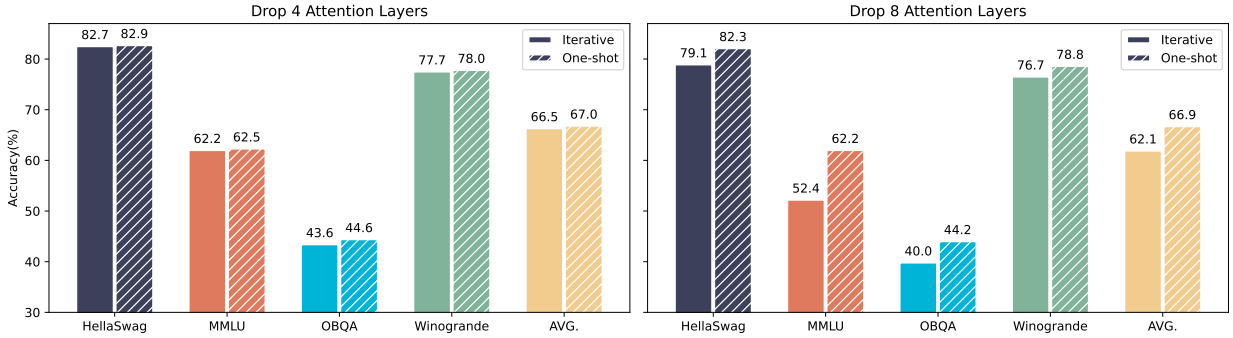

Figure 15: **Ablation Study on Dropping Strategies**, i.e., Iterative and One-Shot, where One-Shot Dropping achieves comparable performance with Iterative Dropping.

Table 6: **Ablation Study on the Residual Connection**, where we report the average performance on MMLU, WinoGrande, HellaSwag, and OpenbookQA. n denotes the number of dropped modules. The notation "w/ res" indicates the involvement of the residual connection, while "w/o" indicates dropping without considering it.

	Attn Drop		MLP Drop	
n	w/o res	w/ res	w/o res	w/ res
4	39.4	65.0	31.2	64.5
8	37.7	65.3	31.1	61.9
12	36.8	65.4	31.1	55.6
16	32.2	63.4	30.8	49.9
20	32.0	62.9	30.9	42.1

Calibration Datasets Figure 3 demonstrates the robustness of the importance scores across different datasets. In Figure 16, we further verify that the importance scores remain relatively stable across various modules of Mistral-7B as the sample size increases. This stability indicates that both Block Drop and Layer Drop maintain consistency regardless of the number of samples. Consequently, we confirm that using 256 samples is sufficient for computing similarity, which serves as the standard adopted for all our experiments.

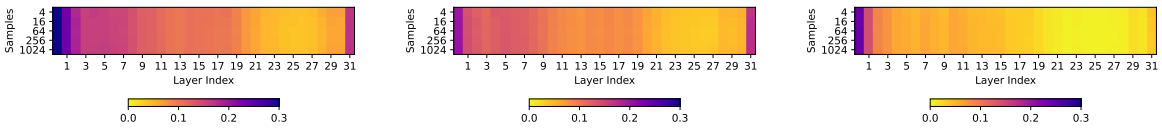

(a) Block (b) MLP (c) Attention

Figure 16: The impact of sample quantity on the importance scores of Block, MLP and Attention.

Comparison with other Compression Techniques We first compare our method with published sparse models pruned by Shortened LLaMA (Kim et al., 2024) in Table 7. Specifically, we prune the original Vicuna-13B-v1.3 model (Chiang et al., 2023) using our proposed Joint Drop technique to maintain the same parameter budget. While Shortened LLaMA involves post-compression retraining, training-free Joint Drop performs better on average performance. We also compare our approach with the mainstream pruning method Wanda (Sun et al., 2023) in Table 8. Under the same parameter budget, our methods outperform Wanda with unstructured sparsity. Additionally, Wanda contributes to fine-grained sparsity, which is not hardware-friendly and has limited practical usage.

Table 7: Comparison with Shortened LLaMA (Kim et al., 2024), where Joint Layer Drop achieves significantly higher speedup.

Method	HellaSwag	MMLU	OBQA	Winogrande	Avg. (↑)	SpeedUp (↑)
Joint Layer Drop	76.0	49.6	42.4	74.9	60.7	1.45
Shortened LLaMA-PPL	75.3	47.7	44.2	74.0	60.3	1.23
Shortened LLaMA-Taylor	76.8	47.0	42.4	76.3	60.6	1.22

Table 8: Comparison with Wanda (Sun et al., 2023) under the same parameter budget. Taking performance into account, we apply unstructured sparsity for Wanda, while our proposed Attention Drop outperforms it in both performance and efficiency.

Method	HellaSwag	MMLU	OBQA	Winogrande	Avg. (↑)	SpeedUp (↑)
Wanda	82.3	54.8	45.2	77.6	65.0	1.00×
Attn-4	82.0	54.7	46.2	77.2	65.0	1.05×
Wanda	82.4	54.7	45.8	77.6	65.1	1.00×
Attn-8	82.2	54.5	47.0	77.4	65.3	1.13×
Wanda	82.4	54.8	46.2	77.4	65.2	1.00×
Attn-12	82.7	54.4	48.0	76.6	65.4	1.20×

D Additional Experimental Results

Tables 9 and 10 present additional results for LLaMA-2-13B and LLaMA-2-70B, which exhibit trends consistent with those observed in Mistral and LLaMA-3.

Table 9: **Experimental Results of Dropping Different Modules**, where we drop the fixed number (e.g., 4 and 8) of modules on Llama-2-13B. Here, Block, MLP, and Attn are corresponding modules. Rows with averaged performance lower than 95% of the original performance are grayed.

Llama-2-13B											
Method	ARC-C	BoolQ	HellaSwag	MMLU	OBQA	PIQA	RTE	WinoGrande	Avg. (↑)	SpeedUp (↑)	γ (↓)
Baseline	59.9	80.7	82.2	55.1	45.6	80.5	65.0	77.0	68.2	1.00×	–
Block-4	54.8	73.3	80.6	54.8	45.8	79.1	60.3	77.5	65.8	1.11×	0.22
Block-8	48.0	56.8	75.3	53.8	41.2	75.3	59.9	75.6	60.7	1.24×	0.31
MLP-4	54.9	76.1	80.4	54.8	45.4	79.5	66.4	77.3	66.9	1.04×	0.32
MLP-8	49.2	63.4	75.6	54.5	42.2	76.0	59.2	75.1	61.9	1.08×	0.79
Attn-4	58.8	80.4	82.0	54.7	46.2	80.5	67.9	77.2	68.5	1.05×	-0.05
Attn-8	58.2	80.5	82.2	54.5	47.0	80.5	64.3	77.4	68.1	1.13×	0.01
Attn-16	56.4	79.2	81.9	48.2	47.4	79.5	59.9	76.2	66.1	1.29×	0.07
Attn-20	53.8	76.9	78.6	51.5	44.4	77.6	59.2	77.1	64.9	1.40×	0.08

Dropping Order on Larger Models We present the dropping order of Block Drop and Layer Drop for the 70B Llama models in Figure 17. Similar to smaller models, larger models also tend to drop deeper layers first. While the dropping order of Blocks differs between Llama-2-70B and Llama-3-70B, we believe this is attributed to different training techniques, e.g., different numbers of training tokens.

Performance on Knowledge Intensive Tasks To assess the impact of Attention Drop on more complex technical tasks, we evaluated Llama-2-7B and Mistral-7B, and two corresponding instruction fine-tuned models, MetaMath-7B-V1.0 and MetaMath-Mistral-7B (Yu et al., 2023). The results in Figure 18 indicate that, except for Llama-2-7B-Math, which is MetaMath-7B-V1.0, all the models do not experience significant performance degradation when dropping fewer than 8 Attention layers. We speculate that this is because Llama-2-7B-Math is initialized with Llama-2-7B and undergoes instruction fine-tuning to improve its mathematical ability. Llama-2-7B-Base exhibits poor performance in mathematics, and the ability obtained solely through fine-tuning appears to be superficial. Therefore, when dropping Attention layers, Llama-2-7B-Math's ability rapidly deteriorates.

Table 10: **Block Drop and Layer Drop on Larger Models**, where we drop a series of numbers (from 4 to 48) of modules on Llama-2-70B. Rows with averaged performance lower than 95% of the original performance are grayed.

	Llama-2-70B										
Method	ARC-C	BoolQ	HellaSwag	MMLU	OBQA	PIQA	RTE	WinoGrande	Avg. (↑)	SpeedUp (↑)	γ (↓)
Baseline	67.4	83.8	87.1	68.5	48.6	82.5	69.3	83.7	73.9	1.00×	–
Block-4	63.8	80.4	84.6	60.2	48.0	81.6	71.1	78.0	71.0	1.07×	0.41
Block-8	59.1	77.5	81.3	55.1	46.2	81.0	68.2	73.2	67.7	1.14×	0.44
Block-16	44.6	64.6	69.9	29.3	40.0	75.2	51.6	59.7	54.4	1.30×	0.65
Block-32	35.1	58.8	56.7	25.7	36.8	71.7	54.5	55.3	49.3	1.67×	0.37
MLP-4	65.4	84.0	86.1	68.7	46.6	82.9	68.2	83.4	73.2	1.04×	0.18
MLP-8	64.4	83.9	84.9	68.7	47.6	81.7	66.8	82.2	72.5	1.05×	0.28
MLP-16	57.5	53.6	81.6	69.1	46.0	79.2	58.8	81.7	65.9	1.08×	1.00
MLP-32	40.6	61.9	64.2	59.8	29.8	64.2	52.7	72.7	55.7	1.17×	1.07
Attn-4	67.2	84.0	87.0	68.6	48.8	82.5	69.3	83.3	73.8	1.06×	0.02
Attn-8	67.3	83.8	86.9	68.5	48.4	82.9	69.0	82.6	73.7	1.12×	0.02
Attn-16	67.8	83.9	87.2	68.5	49.0	83.0	68.2	82.8	73.8	1.21×	0.00
Attn-32	67.2	84.8	87.2	68.4	49.6	81.8	67.5	83.5	73.8	1.35×	0.00
Attn-40	63.7	82.8	84.4	66.2	46.8	80.1	66.8	81.3	71.5	1.48×	0.05
Attn-48	58.5	73.7	80.6	56.8	45.0	79.8	59.6	81.0	66.9	1.62×	0.11

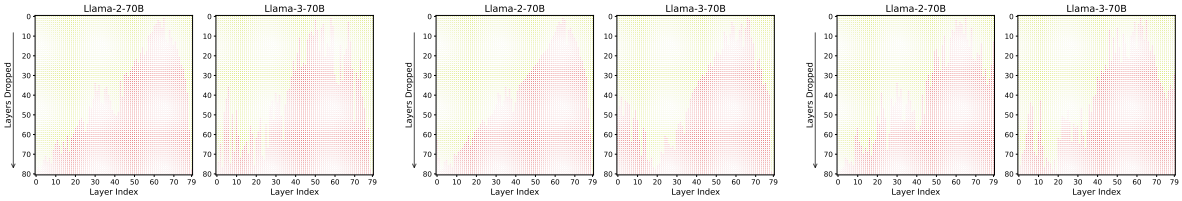

(a) Block (b) MLP (c) Attention

Figure 17: **Visualization of Dropping Order for Block Drop and Layer Drop on Larger Models**, i.e., Llama-2-70B and Llama-3-70B.

We select the first sample from the test set of GSM8K[1] as the input and display the MetaMath-Mistral-7B's raw output in Table 11. Even when dropping 10 attention layers, the model could still give the correct answer of this question, but it failed to adhere to the correct output format. However, when dropping 12 attention layers, the model is no longer able to produce the correct answer of this question. Despite this, post-training offers a potential recovery path for performance loss due to layer dropping. For instance, lightweight LoRA fine-tuning on MetaMathQA significantly boosts Mistral-7B-Math's accuracy from 11.6% to 58.2%, demonstrating its effectiveness and making it a promising avenue for further exploration.

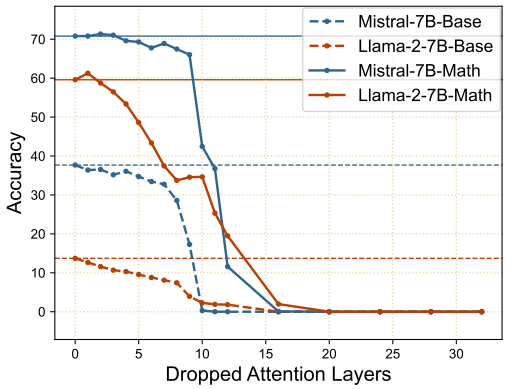

Figure 18: Accuracy Curves on GSM8K.

Attention Drop is Orthogonal to Quantization Given that quantization simplifies data types and enhances efficiency in memory usage and inference speed, we integrate module dropping with quantization to verify whether the quantized models can maintain the performance achieved by Attention Drop. Specifically, we use the mainstream AWQ algorithm (Lin et al., 2024) for 4-bit quantization, following its default settings, which involve using 128 samples from the Pile dataset (Gao et al., 2020) as the calibration dataset.

In Table 12, the integration of quantization still maintains the performance of Attention Drop, i.e., only less than 1% difference in average performance.

[1]https://huggingface.co/datasets/openai/gsm8k

Table 11: **Output Cases of Model with Dropping Some Attention Layers,** where correct answers are marked in green, while incorrect answers are marked in red. Note that "####" is used to extract the correct answer.

Question	Janet's ducks lay 16 eggs per day. She eats three for breakfast every morning and bakes muffins for her friends every day with four. She sells the remainder at the farmers' market daily for $2 per fresh duck egg. How much in dollars does she make every day at the farmers' market?
Golden Answer	Janet sells 16 - 3 - 4 = «16-3-4=9»9 duck eggs a day.\nShe makes 9 * 2 = $«9*2=18»18 every day at the farmer's market.\n #### 18
Method	**Output**
Baseline	Janet's ducks lay 16 eggs per day.\n She eats 3 eggs for breakfast and bakes 4 eggs for muffins, so she uses 3 + 4 = «3+4=7»7 eggs per day.\nTherefore, she sells 16 - 7 = «16-7=9»9 eggs at the farmers' market.\nShe sells each egg for $2, so she makes 9 x $2 = $«9*2=18»18 per day.\n #### 18
Attn-2	Janet's ducks lay 16 eggs per day.\nShe eats 3 eggs for breakfast and bakes 4 eggs for muffins, so she uses 3 + 4 = «3+4=7»7 eggs per day.\nTherefore, she sells 16 - 7 = «16-7=9»9 eggs at the farmers' market.\nShe sells each egg for $2, so she makes 9 x $2 = $«9*2=18»18 per day.\n #### 18
Attn-4	Janet's ducks lay 16 eggs per day.\nShe eats 3 eggs for breakfast and bakes 4 eggs for muffins, so she uses a total of 3 + 4 = «3+4=7»7 eggs per day.\nTherefore, she sells 16 - 7 = «16-7=9»9 eggs at the farmers' market.\nShe sells each egg for $2, so she makes 9 x $2 = $«9*2=18»18 per day.\n #### 18
Attn-6	Janet's ducks lay 16 eggs per day.\nShe eats 3 eggs for breakfast and bakes 4 eggs for muffins, so she uses a total of 3 + 4 = «3+4=7»7 eggs per day.\nTherefore, she sells 16 - 7 = «16-7=9»9 eggs at the farmers' market.\nShe sells each egg for $2, so she makes 9 x $2 = $«9*2=18»18 per day.\n #### 18
Attn-8	Janet's ducks lay 16 eggs per day.\nShe eats 3 eggs for breakfast and bakes 4 eggs for muffins, so she uses a total of 3 + 4 = «3+4=7»7 eggs per day.\nTherefore, Janet sells 16 - 7 = «16-7=9»9 eggs at the farmers' market.\nShe sells each egg for $2, so Janet makes 9 x $2 = $«9*2=18»18 per day at the farmers' market.\n #### 18
Attn-10	The total number of eggs the ducks lay is 16.\nJane eats 3 eggs for breakfast, so there are 16 - 3 = 13 eggs left.\nJane bakes 4 eggs for muffins, so there are 13 - 4 = 9 eggs left.\nJane sells the remaining 9 eggs at $2 each, so she makes 9 * $2 = $«9*2=18}
Attn-12	Dividing the total number of eggs to the number of eggs used for personal use, we get 16 - 3 - 3 = 11 eggs for selling.\nIf each egg is sold for $2, then the total amount earned from selling is 11 * 2 = $22.\nTherefore, she makes $22 every day at the farmers' market.\n #### 22

Attention Drop on Long In-Context Task We evaluate the performance of Attention Drop on the long in-context benchmark. Following LongICLBench (Li et al., 2024), we present the results on BANKING77 (Casanueva et al., 2020), with the only distinction being that we sample 100 examples from the test set. BANKING77 is a banking-domain intent detection dataset comprising 77 classes. We evaluate from 1-shot/label to 5-shot/label, resulting in contextual lengths of 2k, 4k, 7k, 9k, 14k . We employ the togethercomputer/LLaMA-2-7B-32K[2] for Layer Drop, which enlarges the context window of Llama-2 to

[2]https://huggingface.co/togethercomputer/LLaMA-2-7B-32K

Table 12: Integration of Module Dropping and Quantization, "w/Quant" denotes quantized models.

Method	ARC-C	HellaSwag	OBQA	WinoGrande	Avg.
Llama-2-13B					
Baseline	59.9	82.2	45.6	77.0	66.2
w/Quant	59.5	81.7	45.8	77.1	66.0
Attn-4	58.8	82.0	46.2	77.2	66.1
w/Quant	58.0	81.7	46.0	76.2	65.5
Attn-8	58.2	82.2	47.0	77.4	66.2
w/Quant	57.7	81.9	47.0	77.0	65.9
Mistral-7B					
Baseline	61.5	83.2	43.8	78.5	66.8
w/Quant	61.2	82.5	42.8	78.0	66.1
Attn-4	61.0	82.9	44.6	78.0	66.6
w/Quant	61.0	82.8	43.6	77.6	66.3
Attn-8	60.2	82.3	44.2	78.8	66.4
w/Quant	60.1	82.0	43.8	77.5	65.9

Table 13: Performance on Long In-Context Task.

Method	Sequence Length					Avg.
	2k	4k	7k	9k	14k	
Baseline	26	70	75	76	81	65.6
Attn-2	33	68	71	78	77	65.4
Attn-4	28	63	68	75	73	61.4
Attn-6	24	63	65	72	69	58.6
Attn-8	15	50	53	58	64	48.0
MLP-2	29	64	71	70	78	62.4
MLP-4	21	57	64	65	66	54.6
MLP-6	9	41	48	47	48	38.6
MLP-8	11	42	43	48	51	39.0

32k using position interpolation. From the results in Table 13, we observe that Attention Drop maintains performance and outperforms MLP Drop.

Additional Results on Different Normalization Layouts Attention Drop is not restricted to Pre-LN architectures. Adapting to different normalization layouts, including Post-LN or Peri-LN (Pre + Post LayerNorm) (Kim et al., 2025), only requires shifting the measurement point of input/output features. The core logic and pruning criterion of Attention Drop remain unchanged.

While the main experiments in the paper focus on standard Pre-LN models such as LLaMA, we also evaluate Attention Drop on Gemma (Team et al., 2025), which adopts a Peri-LN structure. The results in Table 14 demonstrate consistent redundancy patterns and pruning tolerance, confirming the broader compatibility of our approach across normalization designs.

Table 14: Evaluation of Attention Drop on Gemma models (Peri-LN).

Model	OBQA	PIQA	RTE	WinoGrande	BoolQ	ARC-C	HellaSwag	MMLU	Avg.
Gemma-3-1B	38.4	71.9	68.2	58.6	75.9	40.1	55.9	39.9	56.11
Attn-8	38.6	72.3	68.0	60.1	76.7	37.4	55.5	39.7	56.04
Attn-12	38.0	71.8	68.6	60.0	73.0	38.7	55.0	38.9	55.50
Gemma-3-4B	46.8	76.4	74.0	69.1	84.1	60.4	75.4	58.3	68.06
Attn-8	45.0	78.0	73.1	69.2	83.9	60.1	75.4	57.9	67.83
Attn-12	43.4	75.3	71.4	67.9	82.4	59.8	74.6	56.0	66.35

Magnitude Consideration in Cosine Similarity Our method primarily relies on cosine similarity to identify redundant layers. Although magnitude information is not explicitly included in the criterion, it is implicitly captured through the residual structure. In residual connections $y = f(x) + x$, the cosine similarity between x and y depends on both the direction and the magnitude of $f(x)$; a large $f(x)$ naturally reduces similarity.

Empirically, as shown in Figures 3 and 16, many attention layers exhibit cosine similarity greater than 0.95 or even 0.99. Such high similarity values can only occur when $f(x)$ is both small in magnitude and well-aligned with x, providing strong evidence that these layers are functionally redundant. Furthermore, Figure **??** shows that attention outputs consistently have lower magnitude compared to MLPs, especially in deeper layers, aligning with the trend observed in layer-wise cosine similarity.

While cosine-based ranking may not be the most sophisticated criterion, it is sufficient given the small search space (only L layers) and the competitive performance achieved by the pruned models. Unlike weight- or neuron-level compression, layer-level pruning is a relatively low-complexity problem, where even simple heuristics can be effective and efficient.

Post-Training on Compressed Models Post-training has the potential of recovering the performance degradation caused by Layer Drop. Given computational constraints, we focus on parameter-efficient fine-tuning via LoRA and present the results in Tables 15 and 16. After lightweight fine-tuning, the compressed models exhibit a significant performance recovery. We believe that continual pretraining and full-model fine-tuning can further unlock their potential.

Method	HellaSwag	MMLU	OBQA	WinoGrande	Avg.
Baseline	82.2	65.5	45.0	77.7	67.6
w/LoRA	81.6	65.9	46.6	77.9	68.0
Attn-12	79.4	63.9	42.2	77.8	65.8
w/LoRA	**81.8**	**64.9**	**45.4**	**77.8**	**67.5**
Attn-16	71.2	38.2	39.4	72.8	55.4
w/LoRA	**78.3**	**53.3**	**43.6**	**75.7**	**62.7**
Attn-20	42.2	23.0	30.6	58.7	38.6
w/LoRA	**72.8**	**31.9**	**43.4**	**69.2**	**54.3**

Table 15: Post-Finetuning of Llama-3-8B on Alpaca-GPT4 (Peng et al., 2023a).

Model	Baseline	Attn-8	w/LoRA	Attn-12	w/LoRA
Llama-2-7B-Math	59.6	33.7	**57.5**	19.5	**56.5**
Mistral-7B-Math	70.8	67.5	**68.8**	11.6	**65.2**

Table 16: Post-Finetuning of Llama-2-7B-Math and Mistral-7B-Math on MetaMathQA (Yu et al., 2023).

A Additional Visualization

To provide a comprehensive view of the attention patterns and pairwise token similarity, we present the attention matrices of all attention heads in Figures 20 and 21, along with the token-wise similarity across all layers in Figures 25, 26, and 24.

Randomly Initialized Model Before training, the model has not yet learned how different tokens contribute to lexical or semantic features. In addition, since the model parameters are randomly initialized, attention behaves approximately as an averaging mechanism, i.e., $\mathbf{y}_i = \frac{1}{i}\sum_{j=1}^{i} \mathbf{x}_j W_V W_O$. Noting that attention layers are deployed across stacked blocks, token embeddings are progressively aggregated along the depth of the model. Depending on the magnitude of $W_V W_O$, two scenarios arise: (1) with high magnitude, token embeddings aggregate rapidly, leading to high token-to-token similarity (Figure 25); (2) with low magnitude, limited information flow between tokens results in low similarity among token embeddings (Figure 26). Both scenarios demonstrate the redundancy of attention layers: in the first case, aggregating highly similar tokens provides minimal additional information; in the second, the low magnitude of the attention branch restricts feature updates. Together, these findings reinforce the inherent redundancy of the attention mechanism. As a result, deeper attention layers tend to exhibit excessively high input–output cosine similarity as shown in Figure 19, suggesting potential redundancy.

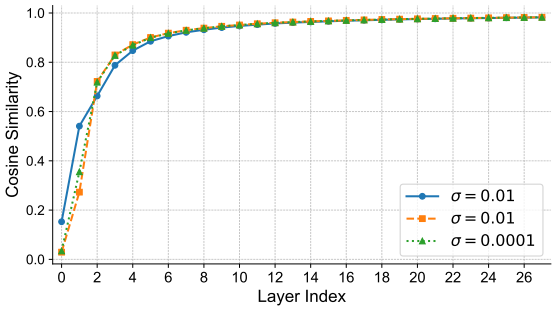

Figure 19: Layer-wise input–output cosine similarity on randomly initialized models with varying values of standard deviations σ.

Pretrained Model With sufficient training, the model learns to identify both lexical and semantic features, with attention sinks emerging at specific tokens (Xiao et al., 2024), which contribute significantly to overall model performance. Moreover, attention sinks in early tokens create an impactful flow of information to later tokens, such that both early and later tokens incorporate the representations of these sinked tokens. This phenomenon enhances token similarity between distant tokens. Despite this, the sparse attention pattern

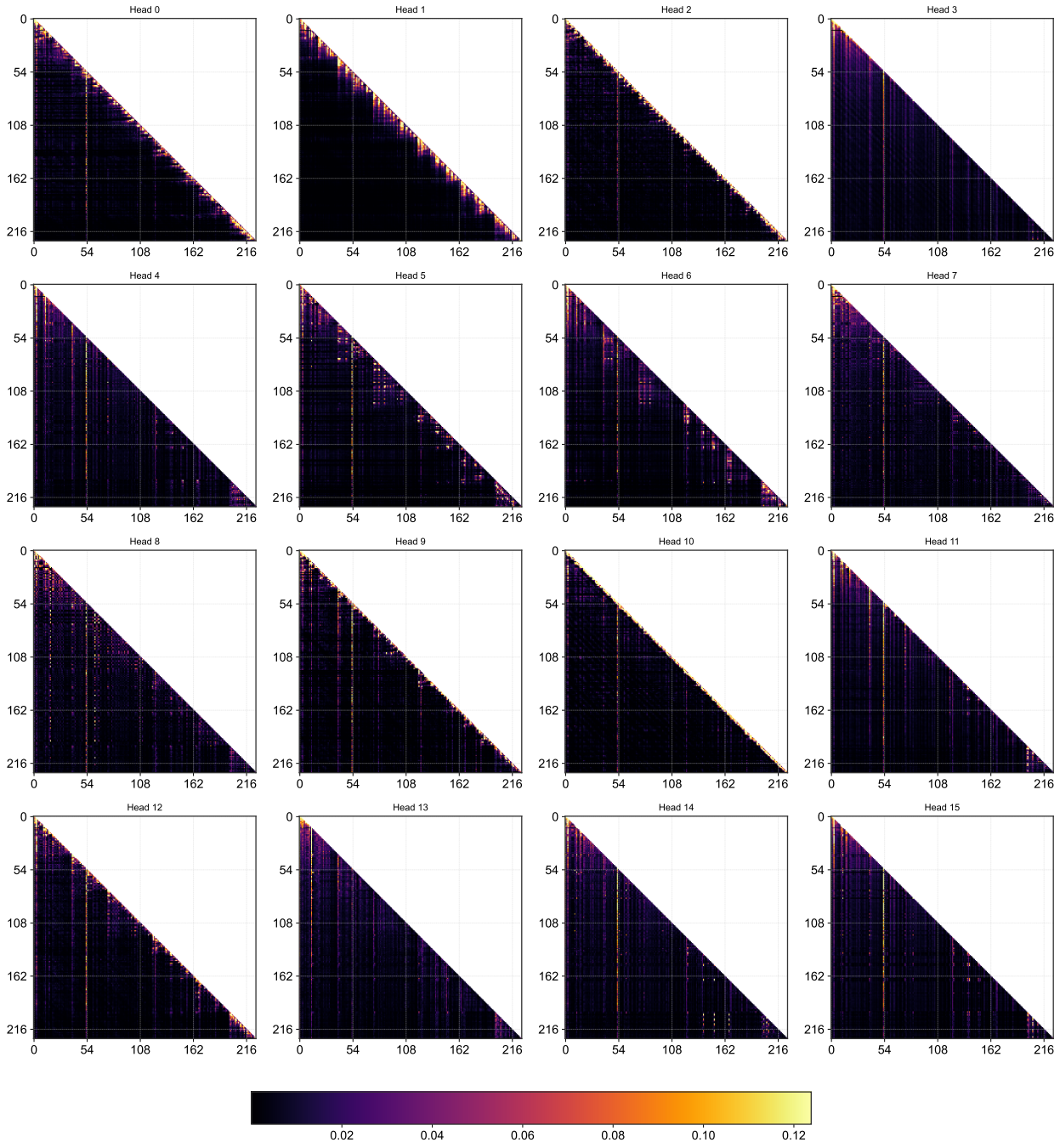

Figure 20: Attention map at the 4-th layer.

introduces redundancy, and the resulting high token similarity at certain depths eliminates the need for some attention operations.

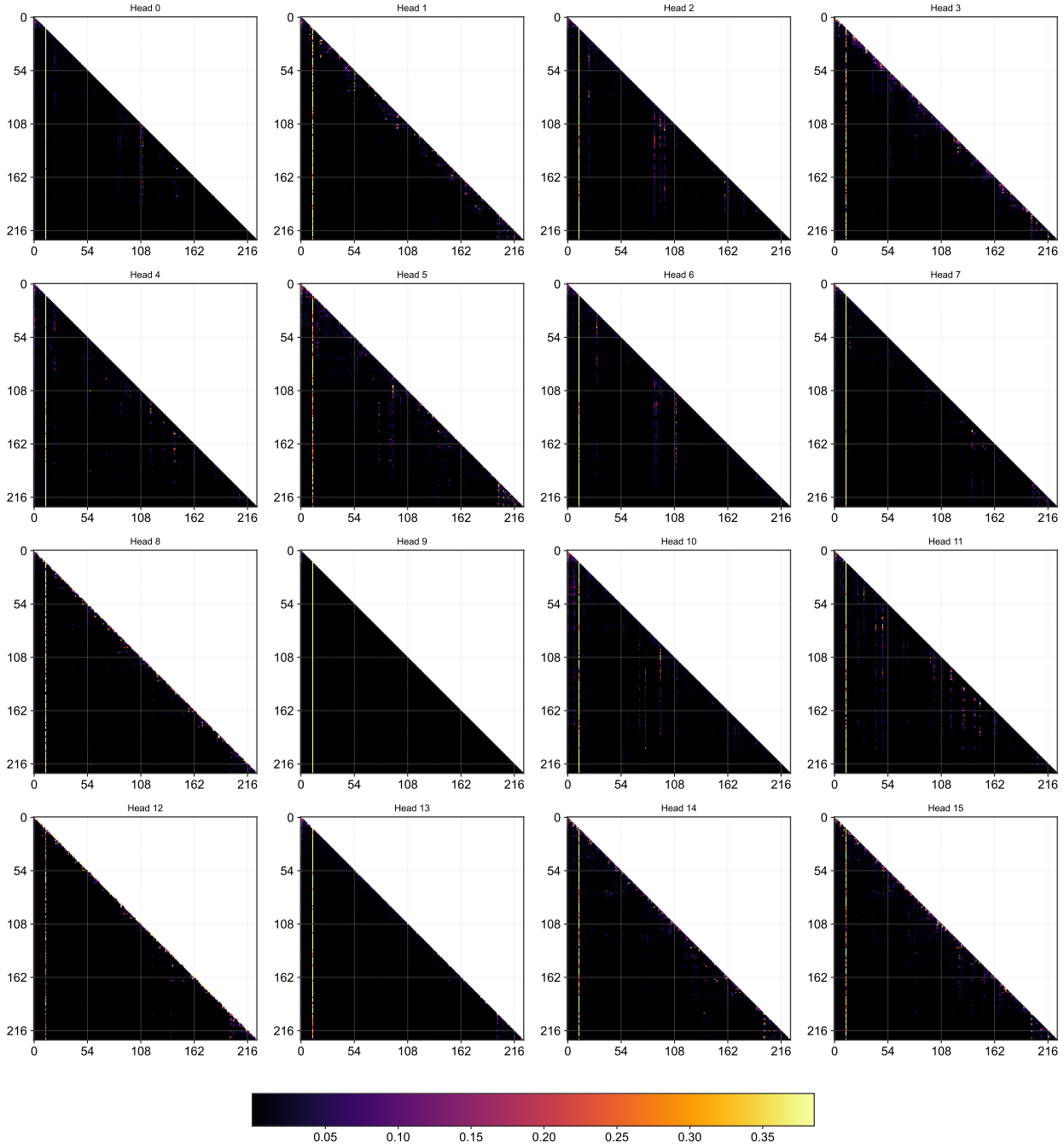

Figure 21: Attention map at the 24-th layer.

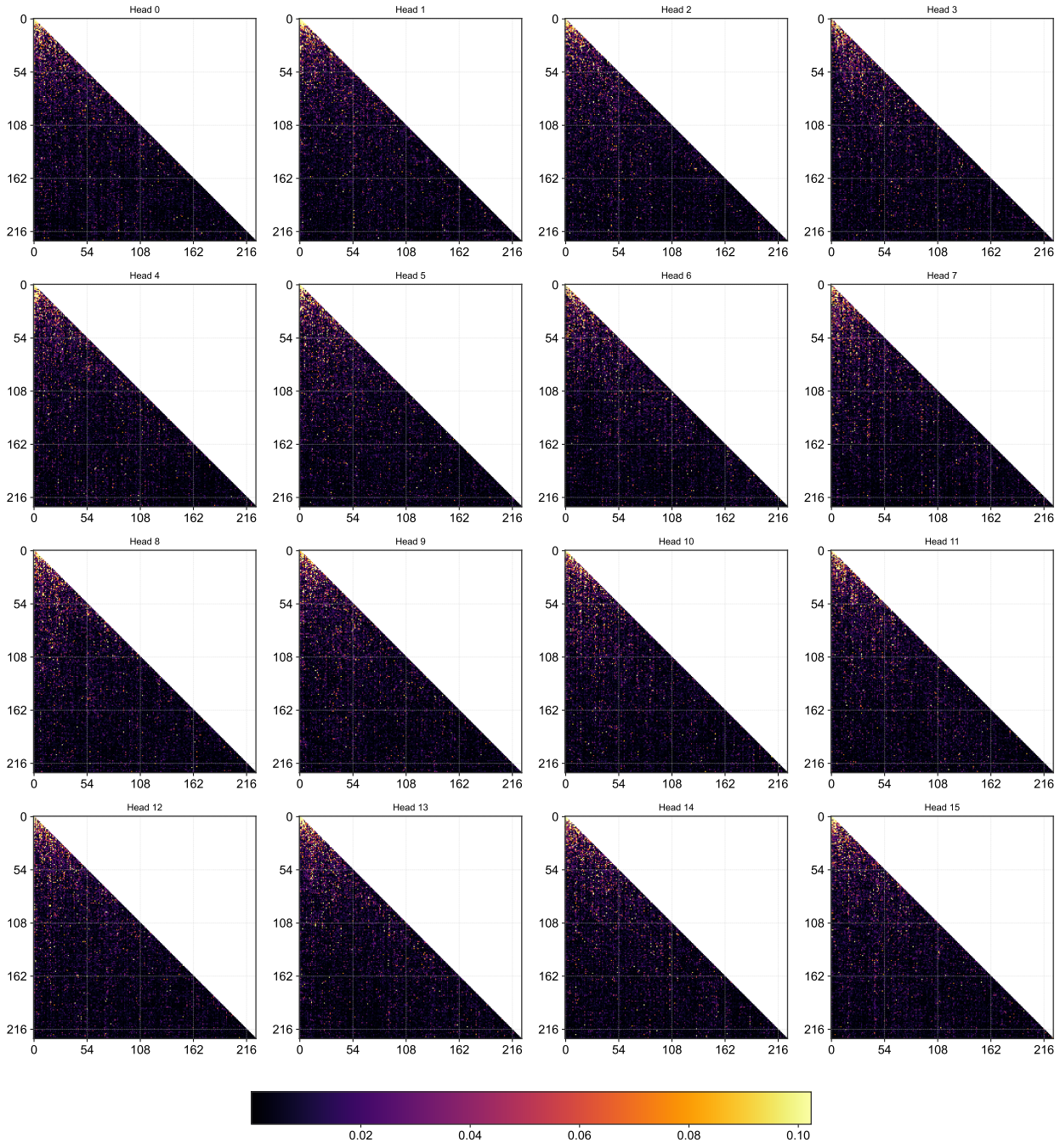

Figure 22: Attention map for randomly initialized map-neo at the 4-th layer.

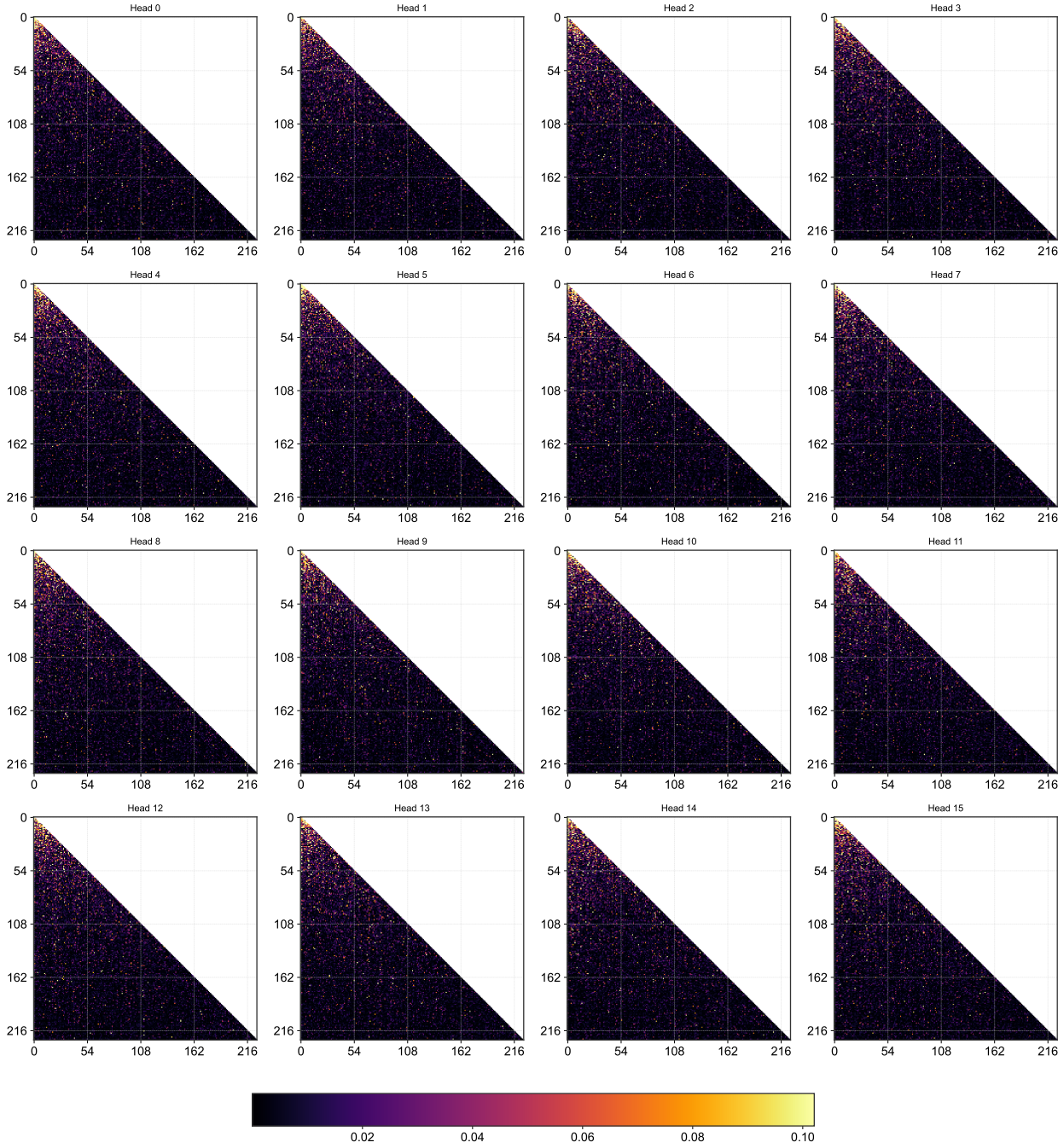

Figure 23: Attention map for randomly initialized map-neo at the 24-th layer.

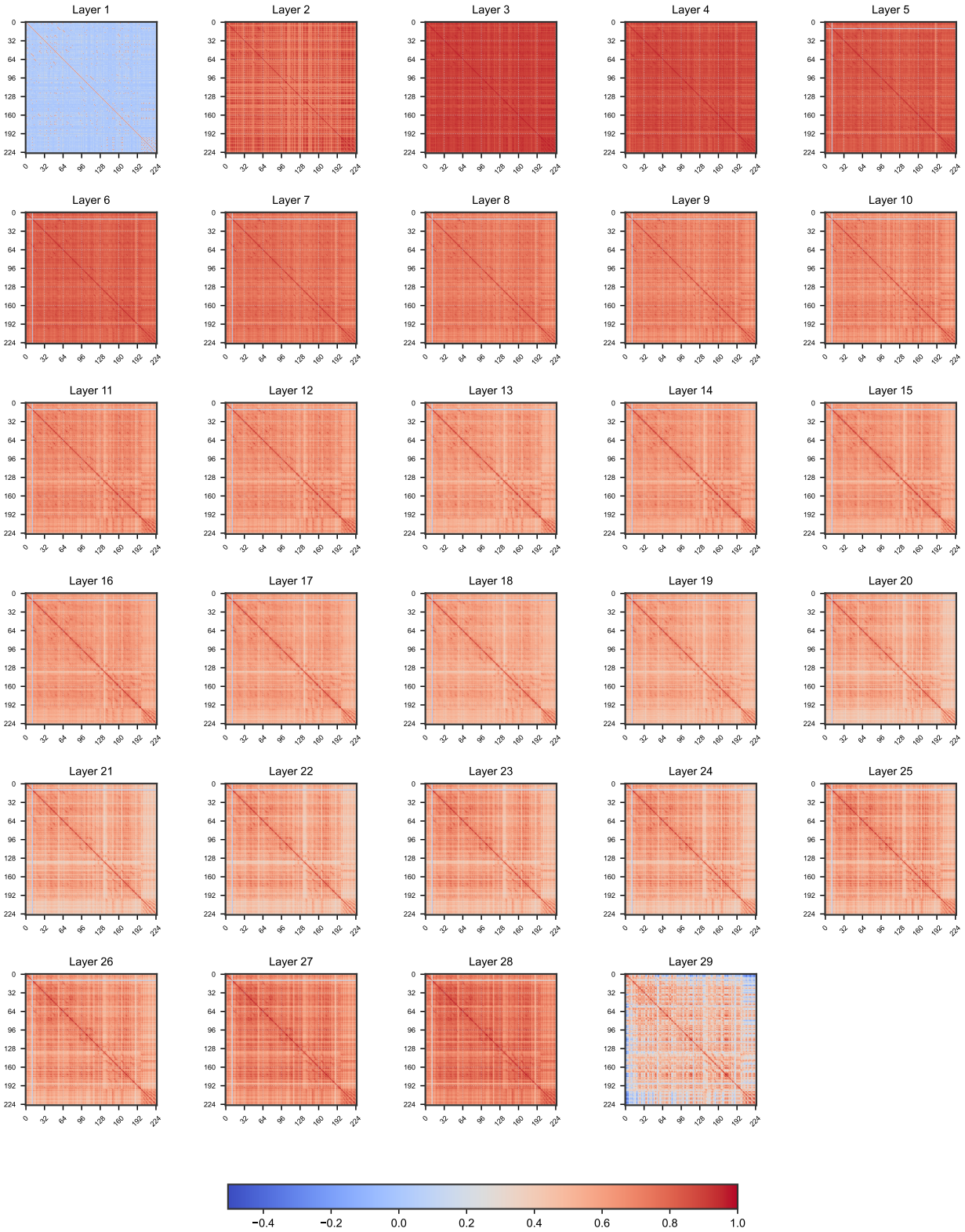

Figure 24: Token-to-token similarity in trained MAP-Neo-7B.

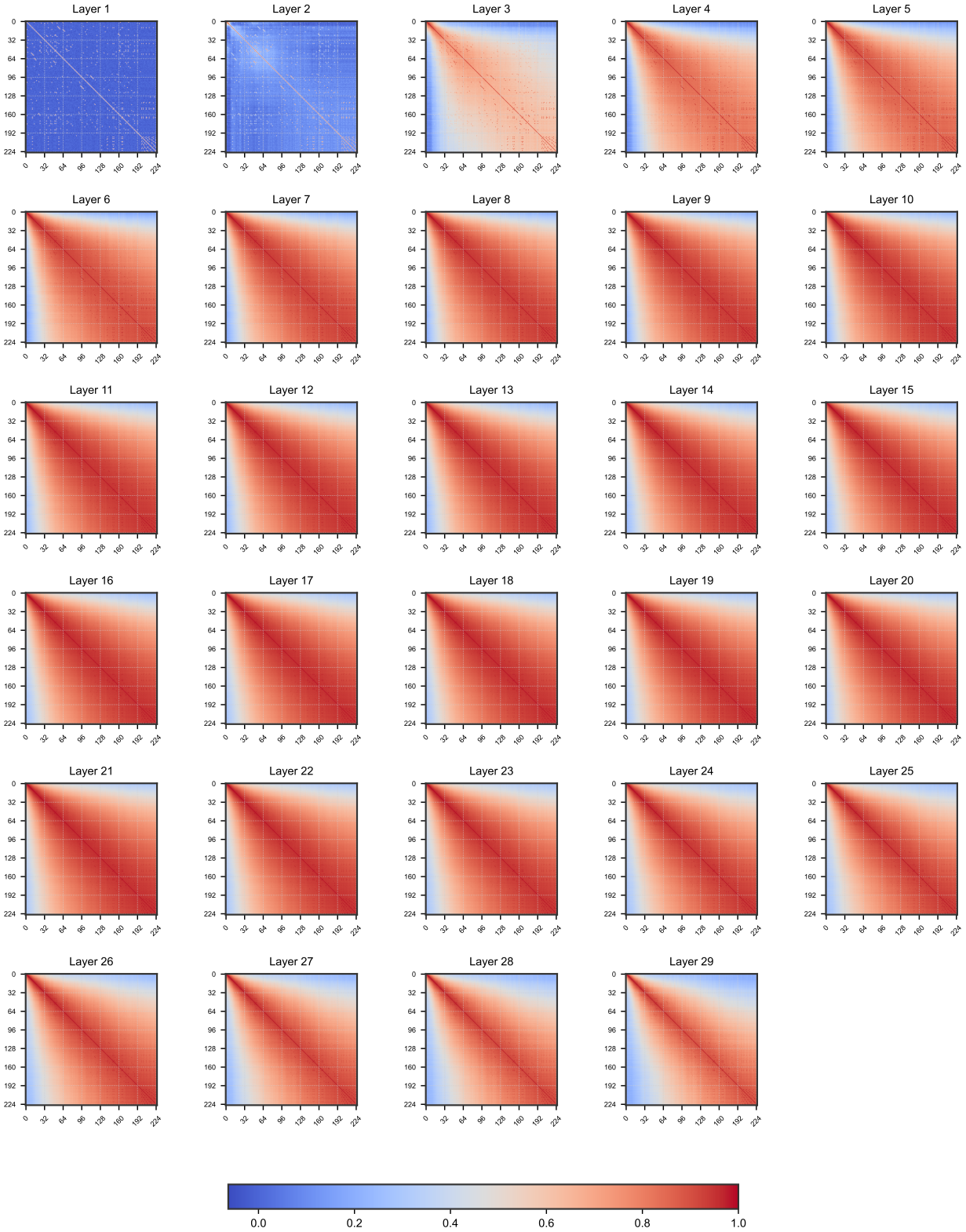

Figure 25: Token-to-token similarity in randomly initialized MAP-Neo-7B, where the parameters of the attention layers are initialized with a high standard deviation of 0.02.

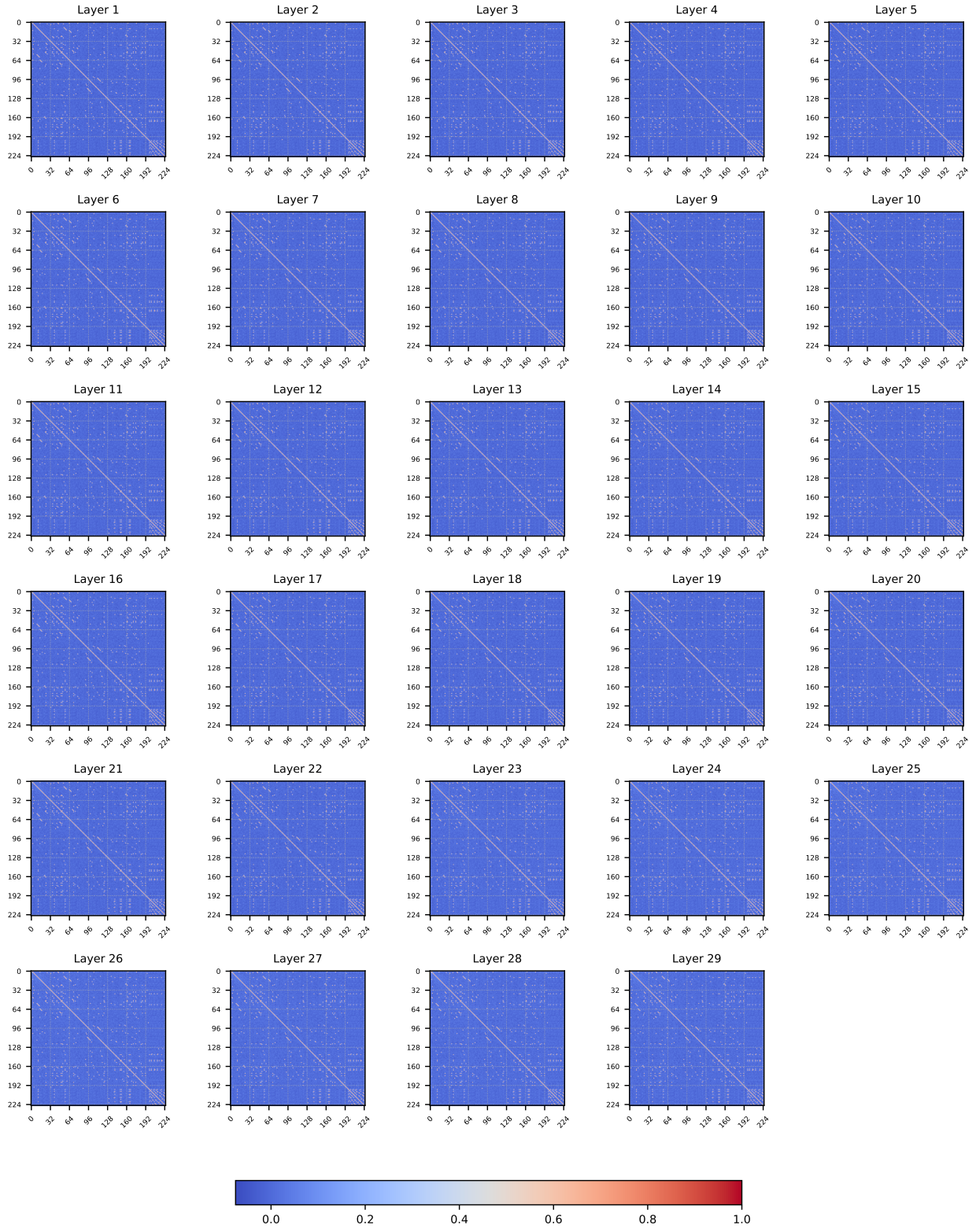

Figure 26: Token-to-token similarity in randomly initialized MAP-Neo-7B, where the parameters of the attention layers are initialized with a low standard deviation of 0.0002.